STRUCTURAL AND MECHANICAL EFFECTS OF INTERSTITIAL SINKS

by

M. J. Klein

Interim Technical Report
8 June 1967 through 8 March 1968

May 1968

Prepared under Contract No. NAS 7-469

Solar, a Division of International Harvester Company

National Aeronautics and Space Administration
Headquarters, Washington, D. C. 20546

NOTICE

This report was prepared as an account of Government sponsored work. Neither the United States, nor the National Aeronautics and Space Administration (NASA), nor any person acting on behalf of NASA

(a) Makes any warranty or representation, expressed or implied, with respect to the accuracy, completeness, or usefulness of the information contained in this report, or that the use of any information, apparatus, method, or process disclosed in this report may not infringe privately owned rights; or

(b) Assumes any liabilities with respect to the use of, or for damages resulting from the use of any information, apparatus, method, or process disclosed in this report.

As used above, "person acting on behalf of NASA" includes any employee or contractor of NASA, or employee of such contractor, to the extent that such employee or contractor of NASA, or employees of such contractor prepares, disseminates, or provides access to, any information pursuant to his employment or contract with NASA, or his employment with such contractor.

STRUCTURAL AND MECHANICAL EFFECTS OF INTERSTITIAL SINKS

by

M. J. Klein

Interim Technical Report
8 June 1967 through 8 March 1968

May 1968

Prepared under Contract No. NAS 7-469

Solar, a Division of International Harvester Company

Available to Government Agencies and Contractors Only

National Aeronautics and Space Administration
Headquarters, Washington, D. C. 20546

Solar Sales Order 6-2426-7

RDR 1534-7

ABSTRACT

The effects of interstitial sinks (reactive metals in which interstitials concentrate) on the interstitial concentration, the structure and the creep behavior of refractory metals were studied. The systems investigated in greatest detail thus far are titanium base interstitial sinks with a columbium base refractory alloy, D43. The systems, Ti/T222, Ti/TZM and Hf/T222, were also studied.

The creep rate of D43 near $0.5T_M$ can be expressed empirically by the Equation

$$\dot{\epsilon} = A\sigma^n e^{-H/RT}$$

where H is 112-118K cal/mole (approximately that for self-diffusion), n is 7.7 to 9.5 and A is $1.7 \times 10^{-2}/C$. The term C included in the definition of A is the concentration of carbon in the alloy in ppm between about 100 and 800 ppm. An interstitial sink reduces the carbon concentration in the D43, thereby increasing the value of A and the creep rate. Electron transmission studies show that this reduction in carbon concentration reduces the number of carbide particles that obstruct dislocation movement. The reduction in the number of these particles correlates with an increase in the creep rate. The values of n and H do not appear to be affected by the action of the interstitial sink.

The grain structures of TZM and T222 specimens annealed with a titanium sink did not differ from the grain structures of specimens annealed without a titanium sink. Although titanium is an interstitial sink for carbon in TZM, it is not a sink for the carbon in T222. A parallel study of the grain structure in T222 exposed to hafnium suggests that this more reactive metal is an interstitial sink for T222.

An experimental method to determine the chemical potential of interstitials in refractory metals was investigated using titanium-columbium alloys. The oxygen concentration in the titanium-columbium alloys was correlated with the free energy of formation of calcium oxide. The method has good potential but additional work will be required to critically evaluate its capabilities.

M. J. Klein
Senior Staff Engineer

Approved by:

John V. Long
Director of Research

A. G. Metcalfe
Associate Director of Research

CONTENTS

ILLUSTRATIONS

ILLUSTRATIONS

TABLES

I. INTRODUCTION

This is the Second Interim Technical Report for Contract NAS-7-469, "Structural Effects of Interstitial Sinks", covering the period June 8, 1967 through March 8, 1968.

In many practical applications it is necessary to use a refractory metal at elevated temperatures in contact with a more reactive metal*. Under these conditions the interstitial elements in the refractory metal tend to concentrate in the more reactive metal (interstitial sink). This partition of interstitials can cause a serious decrease in the elevated temperature strength of the refractory metal. The objective of this study is to obtain a better understanding of the relationships between the changes in interstitial concentration, the structure and the elevated temperature strength of refractory metals when they are placed in contact with interstitial sinks. The combination studied in greatest detail thus far is D43 (Cb-10W-1Zr-0.1C) and a titanium interstitial sink. In future work this investigation will be broadened to include the effect of substitutional solutes on the creep strength of columbium and tantalum base alloys.

The progress during the preceding period is reported in the First Interim Technical Report covering the period June 8, 1966 through June 8, 1967. During this period the effect of the partition of carbon on the structure D43/Ti diffusion couples was studied. Changes in the grain structure of D43 were found to correlate with a reduction in the carbon concentrations in the alloy and an increase in the carbon concentrations in the titanium foil. These structural changes were attributed to the dissolution of structure-stabilizing carbides induced by the migration of carbon to the titanium sink. Calculations based on the equilibrium partition of carbon between titanium and columbium, used to predict the partition of carbon between titanium and D43 were found to agree approximately with experimental results. The calculations predict that the effectiveness of a titanium foil as an interstitial sink is not a sensitive function of its thickness or composition. A series of tests were performed using Ti-Cb alloy foils as interstitial sinks rather than titanium foils. It was found that the alloy foils are effective interstitial sinks even when the concentration of columbium in the foil is relatively high (e.g., Ti-60Cb). Studies were also initiated during the past period to determine the effect of an interstitial sink on the creep life of D43.

---

* Such contacts may arise in brazements, coatings and diffusion bonded joints. Examples are: Hf-20Ta brazed T222 alloy; Ti-Cr brazed D43; (TiCr)-Si coated D43 and Hf-20Ta clad tantalum alloys. The effect may assume critical importance because all high strength refractory alloys use particulate strengthening, e.g., Cb132M, D43, W-Hf-C, TZM, T222 and B88.

During the period covered by the present report the creep behavior of D43 subjected to an interstitial sink was studied further. The creep rate was correlated with the strength of the interstitial sink (its chemical potential), the carbon (carbide) concentration remaining in the alloy and the structure of the alloy. In addition, the effects of titanium and hafnium sinks on the interstitial concentration and the recrystallization of two additional alloys, TZM (Mo-0.5Ti-0.1Zr-0.03C) and T222 (Ta-9.6W-2.4Hf-0.01C) were studied. The work this period was concluded with a brief evaluation of a method to determine the chemical potential of interstitials in refractory alloys. The system investigated was oxygen in columbium-titanium alloys.

Nearly all of the experimental procedures used in this program have been presented in the First Interim Technical Report. Therefore, experimental procedures will be reported in this interim report only when new techniques are involved.

II. CREEP OF D43

D43 is a dispersion strengthened alloy with excellent high temperature creep strength especially in the range 2000 to 2400°F. However, the properties of this alloy that determine its creep strength, and the effect of an interstitial sink on its creep behavior are not known. The objective of this phase of the investigation is to determine the effect of the structure and of an interstitial sink on the creep behavior of D43.

A uniform dispersion of fine stable precipitates is known to enhance the creep strength of metals. However, the effect of the dispersed phase on creep behavior is interrelated with the effects from other structural features such as dislocation networks and subgrains stabilized by the dispersed phase. It is believed that the dispersed phase and the other structural features act as barriers to dislocation movement and to dislocation recovery processes, thereby enhancing creep strength. In past work it was shown that the interstitial sink effect reduces the dislocation networks and the concentration of interstitial phase in D43. Therefore, the interstitial sink effect should also change the creep behavior of this alloy.

It has been shown that the creep of metals is thermally activated; that is, thermal energy must be supplied for creep to occur. In addition, the creep rate is known to be a function of the stress, σ, and the structure, S. Therefore, the elevated temperature creep rate, ϵ°, is often empirically expressed very simply by a rate equation of the form $\epsilon^\circ = f(\sigma, S) \exp -H/kT$, where H is the activation energy k is the Boltzmann constant and T is the absolute temperature. In this regard, creep data are often correlated using the equation,

$$\epsilon^\circ = A \left(\frac{\sigma}{G}\right)^n e^{-H/kT} \qquad (1)$$

where G is the shear modulus, A is a proportionality factor that includes the structure dependency of the creep rate and n expresses the stress dependence of the creep rate. H is usually constant and equal to the activation energy for self-diffusion above $0.5 T_M$ and A is often constant over a range of temperatures although theory indicates that it should vary with temperature. The stress exponent, n, which is found to be about 5 for pure metals is usually decreased by alloying and increased by incorporating a fine dispersed phase into the base metal. Although the stress dependences are usually expressed by a power term as in Eq. 1, the data sometimes conform better to an exponential stress dependency.

The concept of creep is based upon the application of stress and temperature to overcome obstacles to deformation present in the structure; thus the strain rate will be a function of the variables, stress, temperature and structure. Holding two of these variables constant during a creep test will reveal the effect of changes in the third on the strain rate. From measurements of this type the equation governing creep (such as Eq. 1) can sometimes be deduced and related to various creep theories through simplified dislocation models. A determination of the creep equation is thus of both practical and theoretical interest since it can be used to predict the creep rate under different conditions and to yield information concerning the mechanism of creep. Therefore, the creep of D43 was studied before and after subjecting it to an interstitial sink to determine the influence of the sink on the structure, temperature, and stress dependence of the creep rate.

The influence of some of the variables that affect the creep behavior of D43 are discussed in the following sections. Because of the number of these variables and their rather complex dependencies, the subject matter to be discussed is outlined in sequence below.

A. Creep of As-Processed D43 (Sec. 2.1)
   1. Creep curves for the as-processed alloy (Sec. 2.1.1)
   2. The activation energy for creep (Sec. 2.1.2)
      (a) The dependence of the activation energy on creep temperature
   3. The stress dependence of the creep rate (Sec. 2.1.3)
   4. The effect of structure on creep (Sec. 2.1.4)

B. The Effect of an Interstitial Sink on Creep Behavior (Sec. 2.2)
   1. The effect of a titanium sink on creep rates (Sec. 2.2.1)
      (a) Titanium sink in place during creep
      (b) Titanium sink effective before creep
   2. The effect of sink composition on creep rate (Sec. 2.2.2)
      (a) Thermodynamic considerations
      (b) The variations in creep rate with sink composition
   3. The effect of sink compositions on the activation energy (Sec. 2.2.3)
   4. The effect of an interstitial sink on the stress dependence of the creep rate (Sec. 2.2.4)
   5. The relationship between structure, creep rate and sink composition (Sec. 2.2.5)

In the first section (2.1) the influence of processing history, strain, temperature and structure on the creep rate are examined. In the subsequent section (2.2) the effect of an interstitial sink on the creep behavior of D43 is examined and compared with the creep behavior of the alloy prior to subjecting it to an interstitial sink.

For convenience in the discussion, the phase distributed in the D43 matrix as particles will be referred to as carbides although it is realized that this phase (or phases) may be more complex. Structure will refer to both the dislocations and particles in the D43 matrix and the term as-processed or as-received designates the alloy in the condition that it was received from the supplier, i.e., for the Fansteel material, the standard (Std F) or duplex (Dup F) conditions, and for the du Pont material, the duplex (Dup D) condition. For simplicity in the discussion, "creep life" will indicate the time for 8-10 percent strain for the conditions of the test. Most of the data are for a creep temperature of 2200° F. However, some activation energies were determined over a wide range of temperatures.

2.1 CREEP OF AS-PROCESSED D43

The creep characteristics of the as-processed alloy are presented in this section to provide a basis for comparison of the changes in creep behavior induced by an interstitial sink.

2.1.1 Creep Curves for the As-Processed Alloy

The effects of the different processing treatments given the alloy by du Pont and Fansteel on the creep life and the shape of the creep curves at 2200° F are shown in Fig. 1. The creep life of D43 (Dup D) is about four and one-half times longer than that of D43 (Std F) and D43 (Dup F). In addition, the Std F has a longer creep life than the Dup F at strains greater than about four percent. Since the conditions of creep testing were identical and the composition is nominally the same, the dependence of creep life on the processing condition is probably caused by differences in structure induced by processing. The D43 (Std F) has a relatively long region of primary creep (region of decreasing creep rate) extending to ~100 minutes followed by a region of approximately steady state or constant creep rate. The Dup F has a region of slowly increasing creep rate extending to ~100 minutes followed by a region of approximately steady state creep rate (from ~100 minutes to the end of the test), whereas the Dup D has a long region of gradually increasing creep rate extending to ~400 minutes before attaining a steady state creep rate. Probably the most distinguishing feature of these creep curves is the lack of a detectable region of primary creep (region of decreasing creep rate) for the two Duplex specimens.

Steady state creep (constant creep rate) is ordinarily associated with a stable or equilibrium structure for conditions of constant stress and temperature, whereas deviations from a constant creep rate are attributed to dynamic or changing creep structures. On this basis, a longer time is required for the alloy in the Dup D condition to attain a stable structure during creep than is required for the alloy in the Dup F and Std F conditions. The structure of Dup D is initially more creep resistant (lower creep rate) than is its steady state creep structure. This behavior

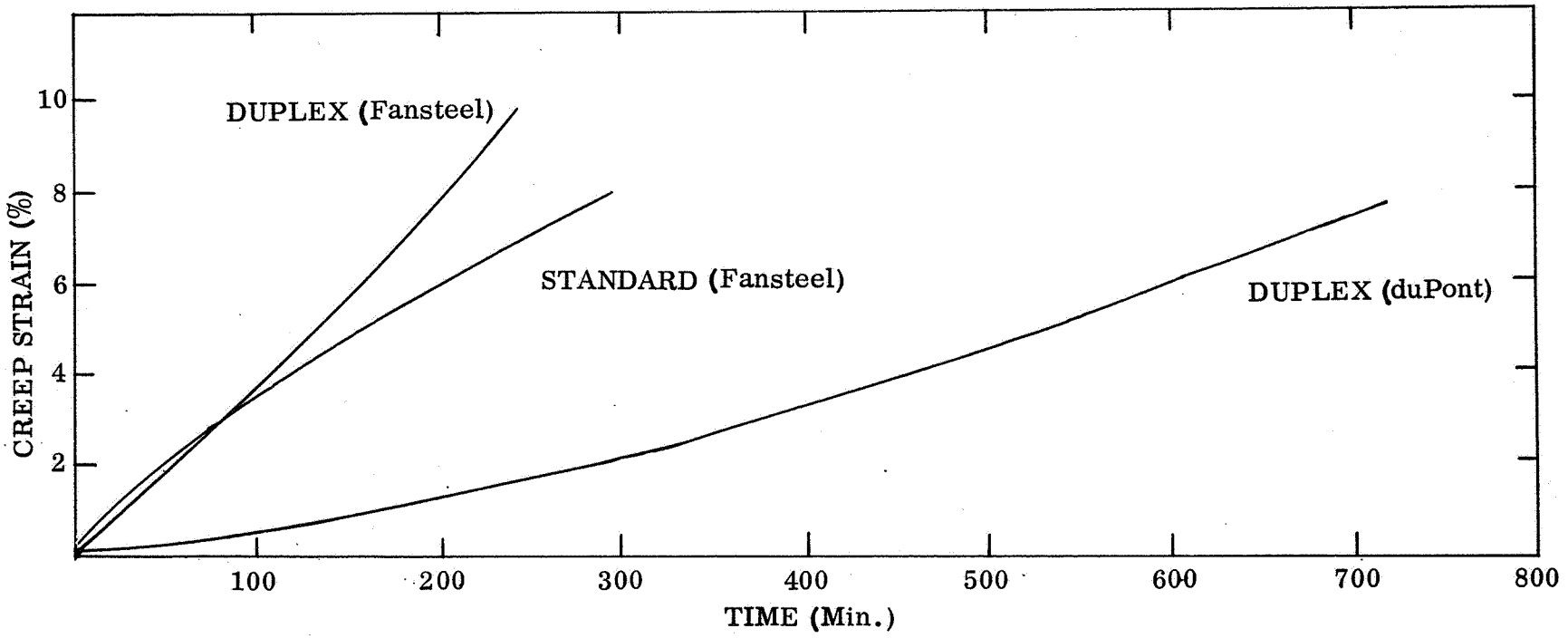

FIGURE 1. THE EFFECT OF PROCESSING ON THE CREEP BEHAVIOR OF D43 AT 2200 F (15,000 PSI)

probably indicates an initial overaging of the as-processed structure at 2200° F, before a stable less creep resistant creep structure is attained. In contrast with this behavior the Std F structure is initially less creep resistant (higher creep rate) than is its steady state creep structure. Thus, creep at 2200° F weakens the stronger Dup D and strengthens the weaker Std F. The initial structure of the Dup F condition does not vary greatly during the test.

As previously discussed (Interim Report June, 1966 - June, 1967) the primary difference between the processing treatments given the Dup D and Dup F material is the higher solution annealing temperature given the former prior to deformation and aging. It is believed that this higher solution annealing temperature will take more carbides into solution so that on subsequent aging more carbides would be reprecipitated. The longer creep life of the Dup D might then be associated with the different carbide distribution and particle size in the Dup D material. Examination of the as-processed alloy using transmission-electron microscopy shows a finer carbide size and a greater coincidence of carbides with dislocations and subgrain boundaries in the alloy in the Dup D condition relative to the Dup F and Std F conditions. The greater number of potential barriers to moving dislocations in the Dup D material may be an important factor contributing to its longer creep life.

2.1.2 Activation Energy for Creep of D43

Activation energies were calculated from the changes in strain rate induced by abrupt shifts in temperature during creep tests. This method has been described in detail in the Interim Report for June, 1966 - June, 1967.

The activation energies were determined for the as-processed D43 (Dup D, Dup F and Std F conditions) as a function of creep strain. The results listed in Table I show that the activation energies are relatively constant with strain. If there is a consistent variation in the activation energy with strain, it is obscured by the scatter in experimental measurements (Standard Deviations for Std F, Dup F, Dup D are 13, 8, and 8 K Cal/Mole respectively). These results suggest that structure differences that may be introduced during creep deformation do not change the mechanism controlling the creep rate of D43. However, the activation energy for Dup D is significantly lower than those for Dup F and Std F. This difference in activation energies may be related to the differences in carbide distribution since a finer carbide was detected in the Dup D material than in the D43 processed in the other conditions. Another possible explanation may be that a difference in the composition of the carbide in the Dup D relative to the carbide in the differently processed material may affect the activation energies for creep. This could occur because the composition of the matrix would be different if the composition of the carbide changes. However, the mechanism by which slight changes in matrix composition could change the activation energies for creep is not clear at this time.

TABLE I

ACTIVATION ENERGY (K cal/mole) FOR CREEP OF AS-PROCESSED D-43 AT 2200°F AS A FUNCTION OF STRAIN

Creep Strain (%)	Std F	Dup F	Dup D
0.8	136	126	82
1.6	131	125	91
2.4	97	123	110
3.2	120	120	94
4.0	128	111	98
5.8	112	127	99
6.6	101	112	89
7.3	113	108	102
8.2	102	115	107
9.0	121	110	95
Averages	116	118	96

The Dependence of the Activation Energy on Creep Temperature

Activation energies were determined for the Dup F material over the temperature range 1600 - 3200°F. The variation in the activation energy as a function of the creep temperature is shown in Fig. 2. A solid line is drawn through the average activation energy values, and the approximate activation energy for self-diffusion in this alloy is indicated in the center of the diagram (Interim Report June, 1966 through June, 1967).

Above about 2200°F ($\sim 0.5\,T_M$) the average activation energy for creep is within the upper range of the approximate activation energy for self-diffusion in this alloy. This agreement is consistent with recovery creep where the creep rate is controlled by a dislocation climb mechanism. During these tests it was observed that the activation energy above 2200 F is independent of the stress within the range of stress values tested (3000 psi to 15,000 psi). This stress independence of the activation energy is also a characteristic of recovery creep where the creep rate is controlled by a dislocation climb mechanism.

Additional work will be required to reduce the scatter in data points below 2200°F. However, the results thus far indicate that for a range of temperature below 2200°F, the activation energy for creep is greater than that for self-diffusion. This is surprising since below about $0.5\,T_M$ the measured activation energy for

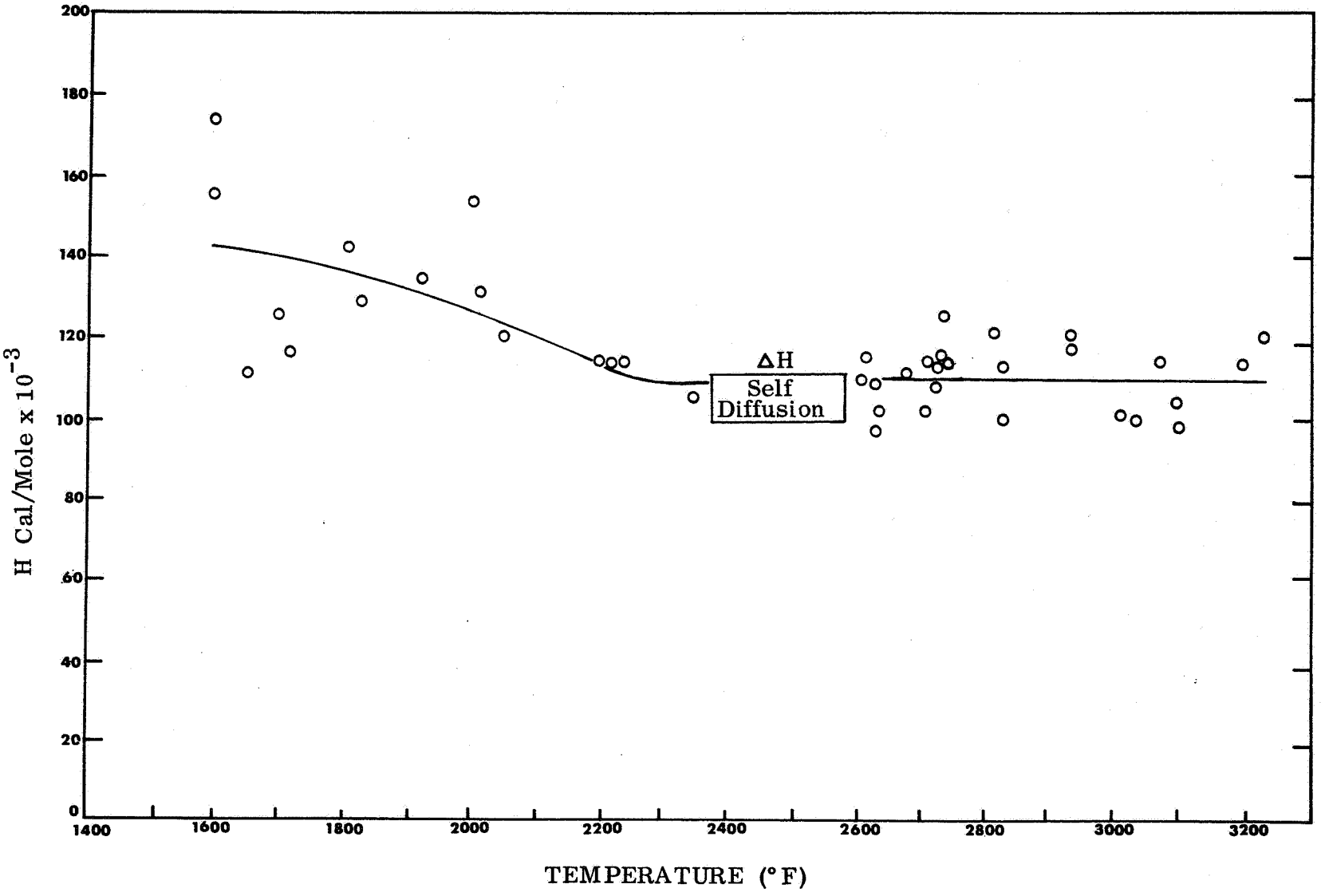

FIGURE 2. THE ACTIVATION ENERGY FOR CREEP OF D-43 AS A FUNCTION OF TEMPERATURE

creep is expected to decrease based on the creep behavior of fcc metals. In this temperature region the measured activation energy, $H^{\#}$ is believed to be stress dependent and to be defined by an equation of the form

$$H^{\#} = H^{\circ} - v\sigma^{\#} \tag{2}$$

where $H^{\#}$ is the measured or apparent activation energy, v is a coefficient of proportionality between stress and energy and $\sigma^{\#}$ is the stress effective in overcoming the energy barrier, H°. Activation energy measurements over a range of temperatures are ordinarily made at low stresses at high temperatures and high stresses at low temperatures so that the strain rate is maintained approximately constant, and the tests can be completed in a reasonable length of time (a procedure followed in obtaining the activation energy values shown in Fig. 2). According to Eq. 2, $H^{\#}$ will thus decrease with decreasing temperatures because $\sigma^{\#}$ is increased. This is in contrast with the experimental results shown in Fig. 2 where $H^{\#}$ increases with decreasing temperature despite an increase in stress of from 15,000 psi at 2200° F to 44,000 psi at 1600° F.

The increase in $H^{\#}$ below 2200° F could be accounted for if solute atoms interact with dislocations in this temperature region and affect their mobility. The activation energy for creep deformation may then reflect the energy required for a dislocation to overcome its atmosphere of solute atoms in addition to the normal barriers to dislocation movement.

The conditions of temperature and strain rate under which an interaction between solute atoms and moving dislocations can be expected has been analyzed by McLean (Ref. 1) and Cottrell (Ref. 2). An approximate relationship can be derived by equating the mobility of the solute atoms (the first term in the Eq. 3) to the velocity of the dislocations (the second term in Eq. 3) so that

$$\frac{\sigma b^2 D}{10kT} = \frac{\epsilon^{\circ}}{\rho b} \quad . \tag{3}$$

In this equation σ is the stress, b is the Burgers vector, k is the Boltzmann constant, T is the temperature, ϵ° is the strain rate, ρ is the dislocation density and D is the diffusion coefficient.

Where $\rho = 10^9$, $b = 2.5 \times 10^{-8}$ cm, $\sigma = 10 \times 10^8$ dynes/cm^2 (about 15,000 psi) and T = 1365° K (~ 2000° F),

$$D = 1 \times 10^{-7} \epsilon^{\circ}. \tag{4}$$

Since H/kT in the diffusion equation is approximately equal to $17T/T_M$ and the frequency factor is about unity,

$$\frac{T}{T_M} = \frac{17}{16 - \ln \dot{\epsilon}^\circ} \quad . \tag{5}$$

Equation (4) and (5) thus express very approximately the conditions of strain rate and temperature where interactions between substitutional solute atoms and moving dislocations could lead to an increase in the activation energy for creep as previously described.

For D43, where $\dot{\epsilon}^\circ = 7 \times 10^{-6}$/sec (the approximate $\dot{\epsilon}^\circ$ used in these tests) and interaction between substitutional elements and dislocations would be expected to occur according to Eq. (5) at $0.6\,T_M$ or about 2650° F. In this regard, Eq. (5) is not a sensitive function of the assumed parameters, e.g., an increase in ρ to 10^{10} decreases T/T_M to 0.56. Thus for reasonable values of the parameters the temperature derived from Eq. (5) is considerably higher than the temperature in Fig. 1 (about 1800° F or $0.44\,T_M$) at which the activation energy appears to rise above that for self-diffusion. The increase in activation energy is not likely to be caused by interstitial interactions with dislocations because of the high mobility of interstitials in this temperature range. The apparent diffusivity of the element responsible for the increase in activation energy below 2200° F in D43 can be calculated according to Eq. (4) for the strain rate used in these tests. Where $\dot{\epsilon}^\circ$ is 7×10^{-6}/sec, D is approximately $10^{-12}\,cm^2$/sec. The interaction is probably not due to the diffusion of Zr that may be in solution in D43 since its diffusivity at 1800° F in Cb is reported to be $\sim 10^{-17} cm^2$ sec (Ref. 3). The diffusion of W in D43 will probably be even slower than Zr so that it is not likely to account for the increase in the activation energies. Therefore, some more complex diffusing species must account for the observed results. In this regard, where clustering of solutes affects their mobility or where solutes interact with each other, as well as with dislocations, the temperature range of the interaction may be shifted or broadened according to the mobility of the diffusing species.

2.1.3 The Stress Dependence of the Creep Rate of As-Processed D43

The stress dependency of the creep rate was examined at 2200° F for the alloy in the various as-processed conditions. Stress dependencies were determined by measuring the change in strain rate before and after sudden shifts in stress during creep tests. A typical differential stress test is shown in Fig. 3, and the strain rates derived from this test are listed in Table II. It is evident that the stress dependency of the strain rate for this alloy is approximately independent of the stress and strain history of the specimen, e.g., the strain rate for 15 ksi is reproducible (within experimental error) at the beginning and end of the creep test. In this regard, it was found that the stress shift method yielded approximately the same strain rate

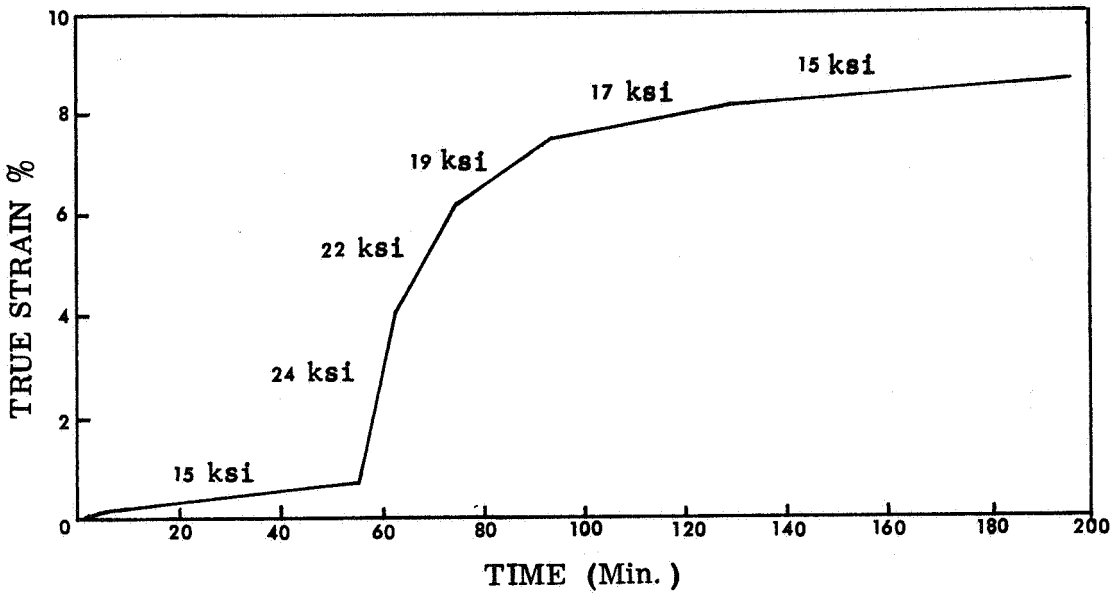

FIGURE 3. TYPICAL SEQUENCE FOR DIFFERENTIAL STRESS TESTS AT 2200° F PRECREEP TREATMENT 57 HRS AT 2200 °F

TABLE II

CHANGE IN CREEP RATE OF D43 WITH STRESS FOR DIFFERENTIAL STRESS TESTS AT 2200° F

σ (KSI)	15	24	22	19	17	15
ϵ (%)	0 - 0.7	0.7 - 4.0	4.0 - 6.5	6.5 - 7.7	7.7 - 8.5	8.5 - 9.0
$\dot{\epsilon}$ /Min x 10^3	0.15	6.9	3.4	0.93	0.37	0.14

dependency as that derived from a series of single stress creep tests. This is shown in Fig. 4 where the results from a number of differential stress tests and single stress test are plotted together. The results show that the strain rate, $\dot{\epsilon}$, is approximately proportional to σ^n (within the range of stress tested) where σ is the stress and n is a constant of about 9.5. It should be pointed out, however, that the data can also be adequately described by the relationship $\dot{\epsilon} \alpha e^{B\sigma}$ where B is about 0.6×10^{-3} psi^{-1} (Fig. 5). Unless the range of isothermal stress variations is large it is difficult to establish which of these empirical relationships is more applicable to the data. For example, if the data are linear for a plot of $\ln \dot{\epsilon}$ versus $\ln \sigma$ i.e., $\dot{\epsilon} \alpha \sigma^n$ where n= 9.5 over a stress range of 15 to 20 ksi the data will also be approximately linear for $\ln \dot{\epsilon}$ versus σ, i.e., $\dot{\epsilon} \alpha e^{B\sigma}$. Here, B, the slope of the latter plot will vary from

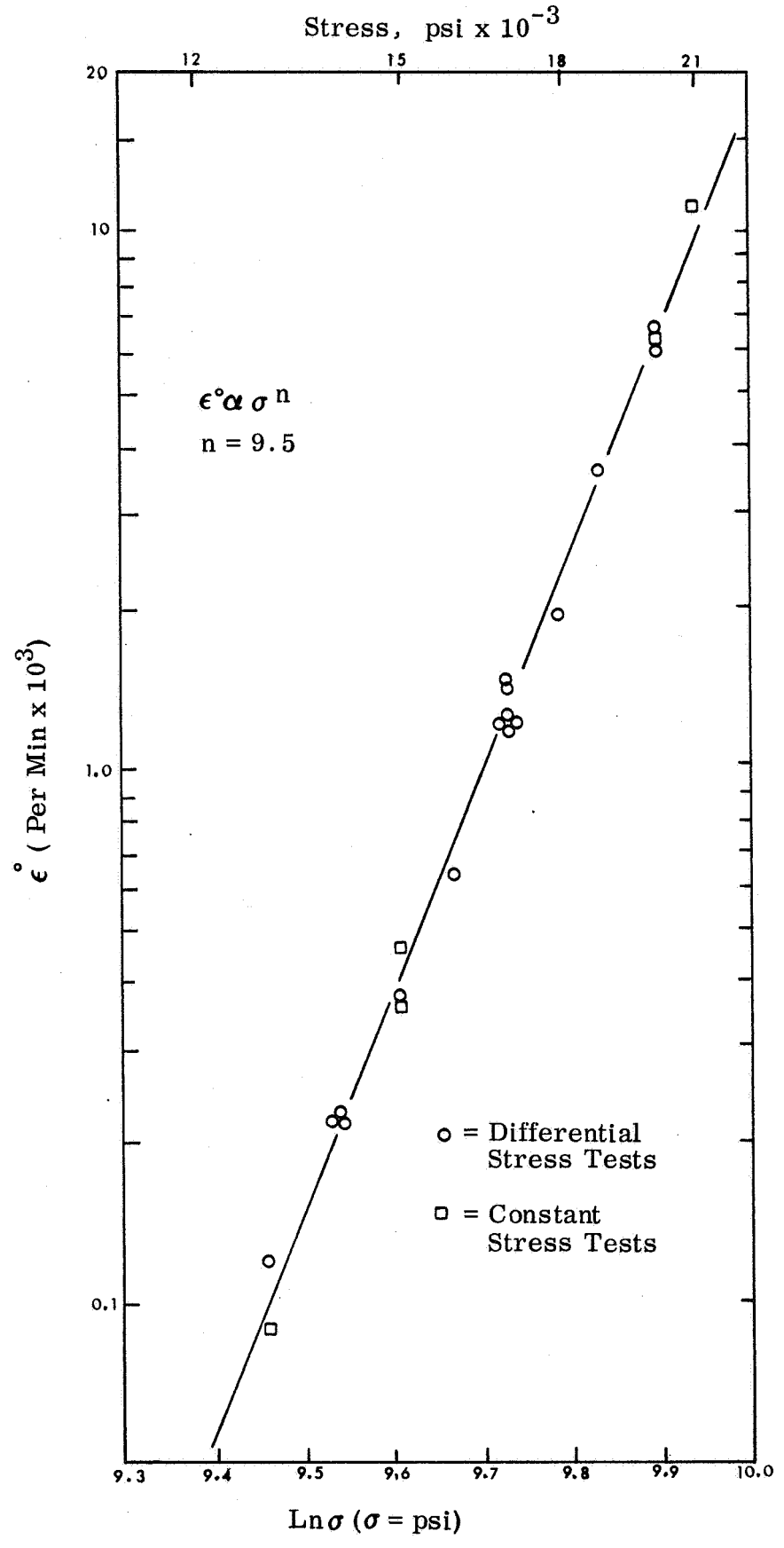

FIG. 4. THE STRESS DEPENDENCE OF THE STRAIN RATE AT 2200°F FOR D43 (DUP F)

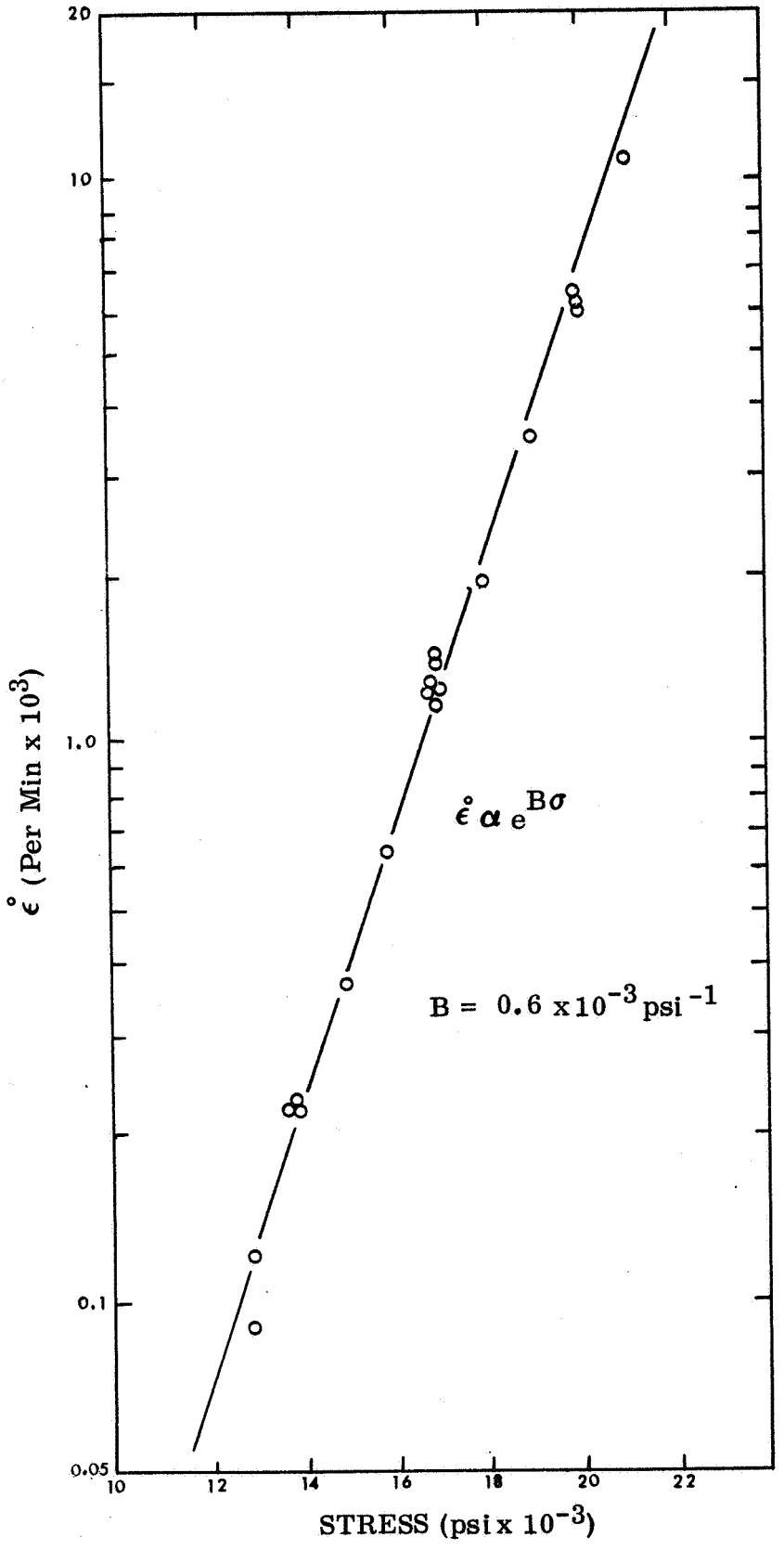

FIGURE 5. THE STRESS DEPENDENCE OF THE STRAIN RATE D43 (DUP F) AT 2200° F

$0.63 \times 10^{-3} psi^{-1}$ to $0.48 \times 10^{-3} psi^{-1}$ over this range of stress variations. This rather small change in slope may be difficult to distinguish from the scatter in experimental data points.

The relationships between B and n can be derived as follows. For data conforming to the equation

$$\dot{\epsilon} = C\sigma^n \tag{6}$$

where C and n are constants

$$\frac{d\dot{\epsilon}/\dot{\epsilon}}{d\sigma/\sigma} = n.$$

and for data conforming to the equation

$$\dot{\epsilon} = Ae^{B\sigma} \tag{7}$$

where A and B are constants,

$$\frac{d\dot{\epsilon}/\dot{\epsilon}}{d\sigma/\sigma} = \sigma B$$

Therefore

$$n = \sigma B \tag{8}$$

and

$$A/C = (\sigma/e)^n.$$

Thus, for data that obey Eq. 6, where C and n are constants, B and A in Eq. 7 must vary according to the relationships

$$B = n/\sigma$$

and

$$A = C(\sigma/e)^n$$

Although either Equation 6 or 7 appears to adequately describe the stress dependence of the creep rate for D43, the σ^n relation will be used in the remainder of this report. This will facilitate comparison with most published work since steady state creep rates are most often expressed in terms of a σ^n dependency.

Fig. 6 shows the stress dependence of the strain rate at 2200° F for the differently processed D43. Although the processing treatment affects the creep rate as

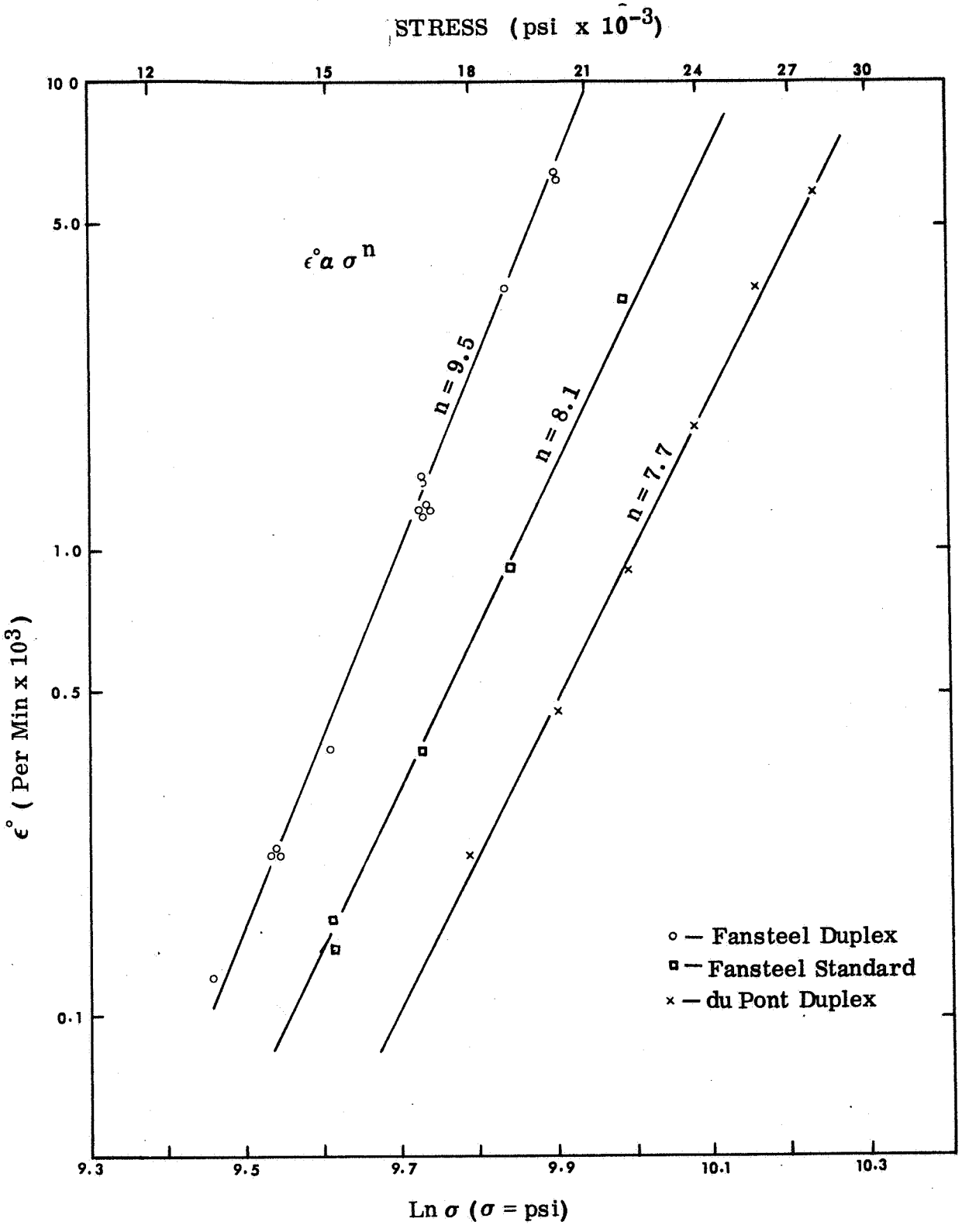

FIGURE 6. THE EFFECT OF PROCESSING ON THE STRESS DEPENDENCE OF THE STRAIN RATE AT 2200° F

previously discussed, these results show that processing has only a minor effect on the stress dependence of the creep rate. The du Pont Duplex condition has the lowest stress exponent ($n = 7.7$) and the Fansteel Duplex has the highest stress exponent ($n = 9.5$). This difference, although small, is judged to be greater than the experimental variation in the value of n of about ± 0.5.

2.1.4 The Effect of Structure on Creep of As-Processed D43

In this section the structures as revealed by transmission electron microscopy are compared before and after creep testing to gain some insight into the effect of carbide particles on the elevated temperature strength to this alloy. Creep specimens were cooled from the creep temperature with the load on the specimen to retain the elevated temperature dislocation structures for subsequent examination.

The structures observed in the as-processed D43 prior to creep testing have been discussed in detail in the First Interim Technical Report. Thus, the precreep structures will only be briefly considered here for comparison with the structures observed in the specimens after creep testing. In general, all of the as-processed structures prior to creep testing (Dup D, Dup F, Std F) are inhomogeneous, having a range of subgrain sizes (300-3000Å) and variations in the carbide particle sizes (1-10 microns) and distributions. For a general comparison with the post-creep structures to be discussed here, the as-processed structure of D43 (Std F) prior to creep testing is shown in Fig. 7A and typical structures after creep testing are shown in Figures 7B and 8. After creep, the structures are characterized by the elimination of many of the subgrains observed in the as-processed material. The subgrains remaining in the specimens after creep are in general larger than those in the as-processed structure. In addition, the dislocations are more uniformly distributed after creep, and they nearly all lie along carbide particles. These results suggest that the carbide particles enhance the creep strength of D43 by interacting with moving dislocations. There is no evidence for an indirect dislocation particle effect such as might be derived from the formation or retention of a particle-induced stable subgrain structure which, in turn, could obstruct the movement of dislocations.

As previously discussed, a dispersed phase can impart elevated temperature strength to a metal by interacting with dislocations so that their movement or generation is obstructed. Deformation can continue if dislocations deform or fracture particles leaving loops behind (Orowan mechanism) or by-pass particles by cross-slip or climb. Carbide particles can thus alter the dislocation structure in a number of ways even though only one mechanism may be rate controlling. Therefore, it is difficult to deduce the rate controlling dislocation mechanism from structural observations alone. However, the structure must, nevertheless, be consistent with the actual dislocation movements in the lattice and their interactions with the particles. For example, the structure in the specimens after creep shows no definite evidence of deformation or fracture of the carbide particles induced by dislocation movements. In addition, dislocation loops around particles as postulated by Orowan were not observed. However,

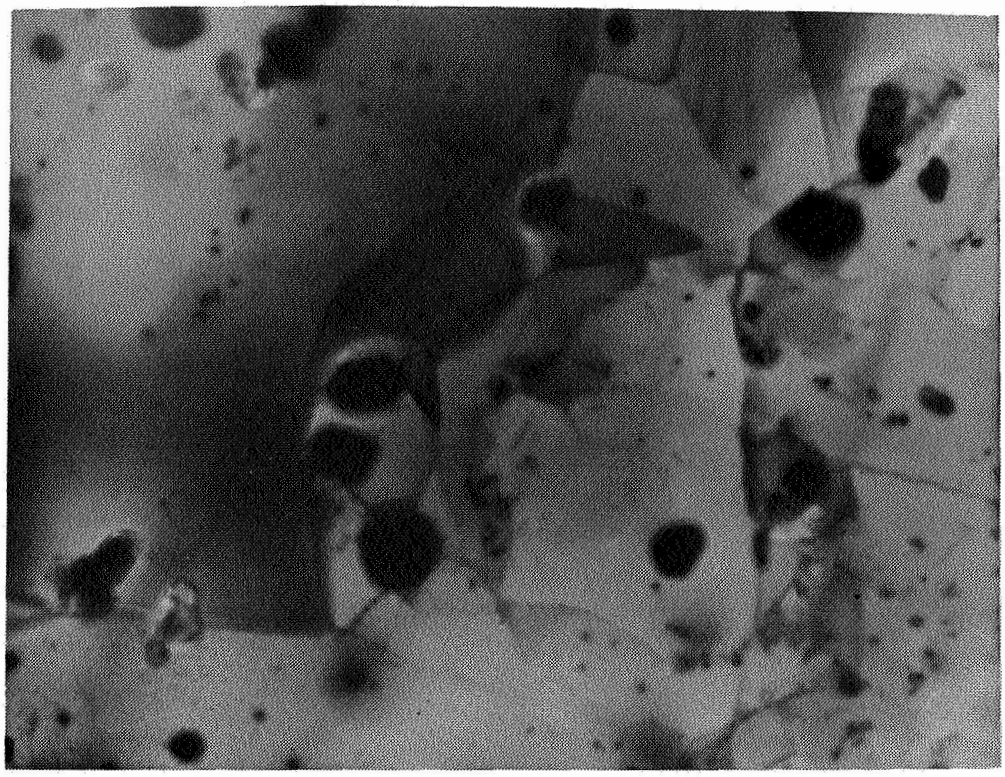

A. Before Creep

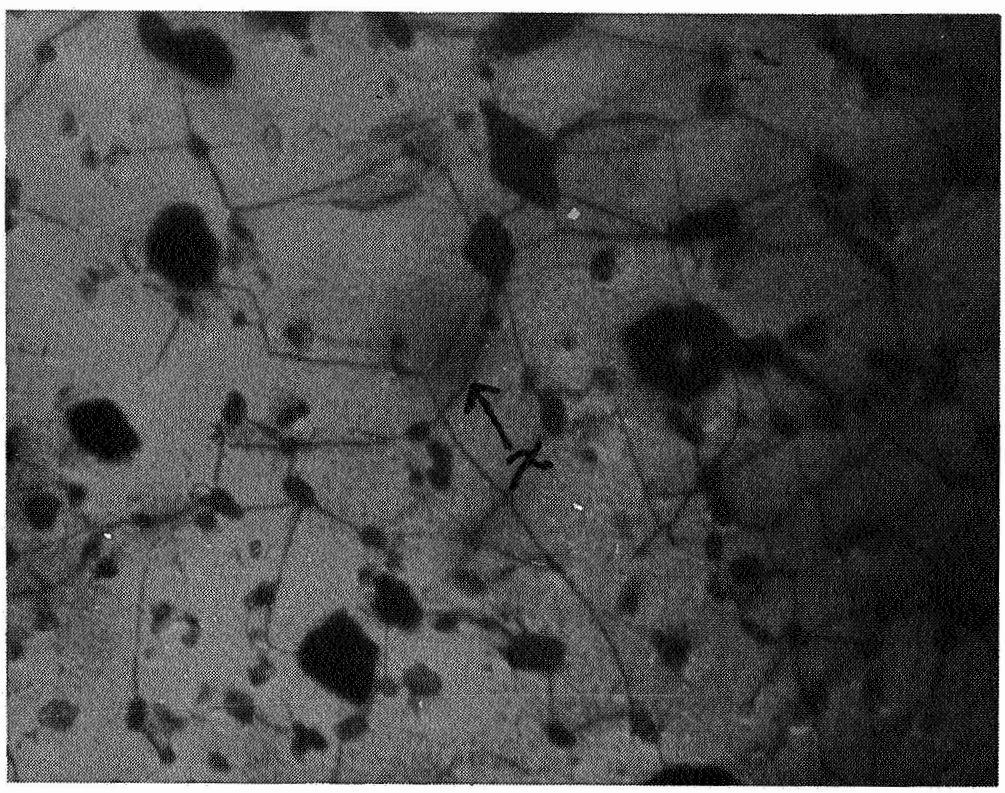

B. After 9 Percent Creep Strain

FIGURE 7. STRUCTURE OF AS-RECEIVED D43 (STD F): 32,000 MAGNIFICATION

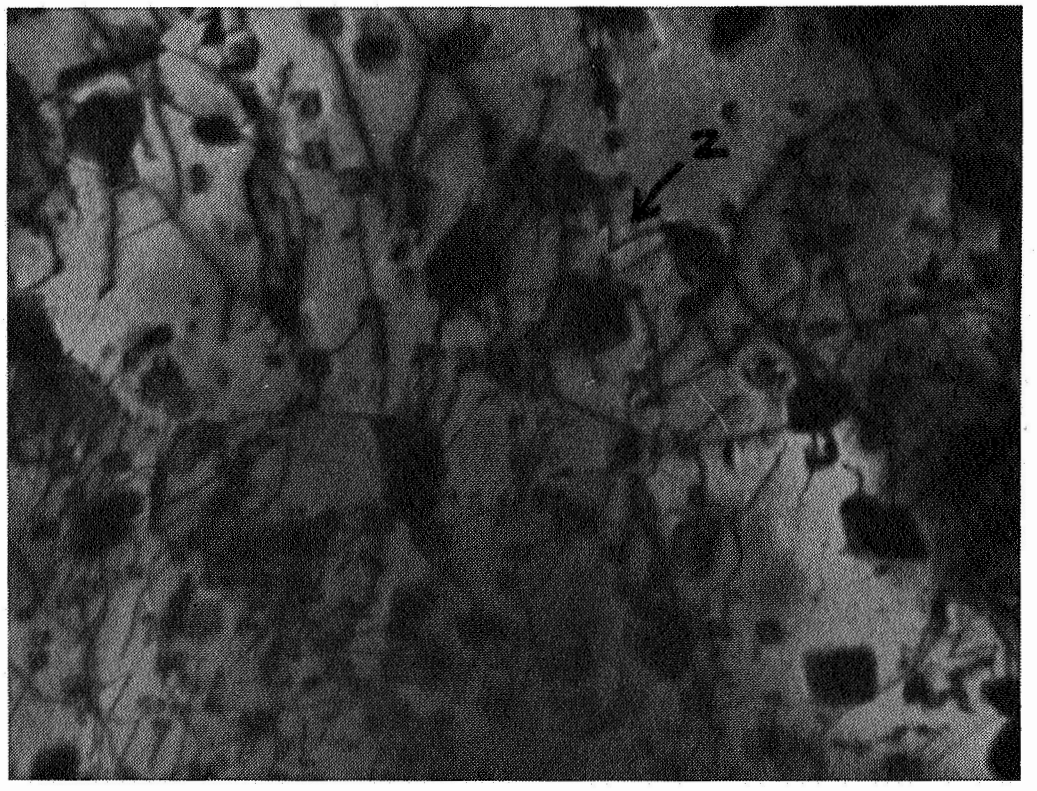

A. Dup F

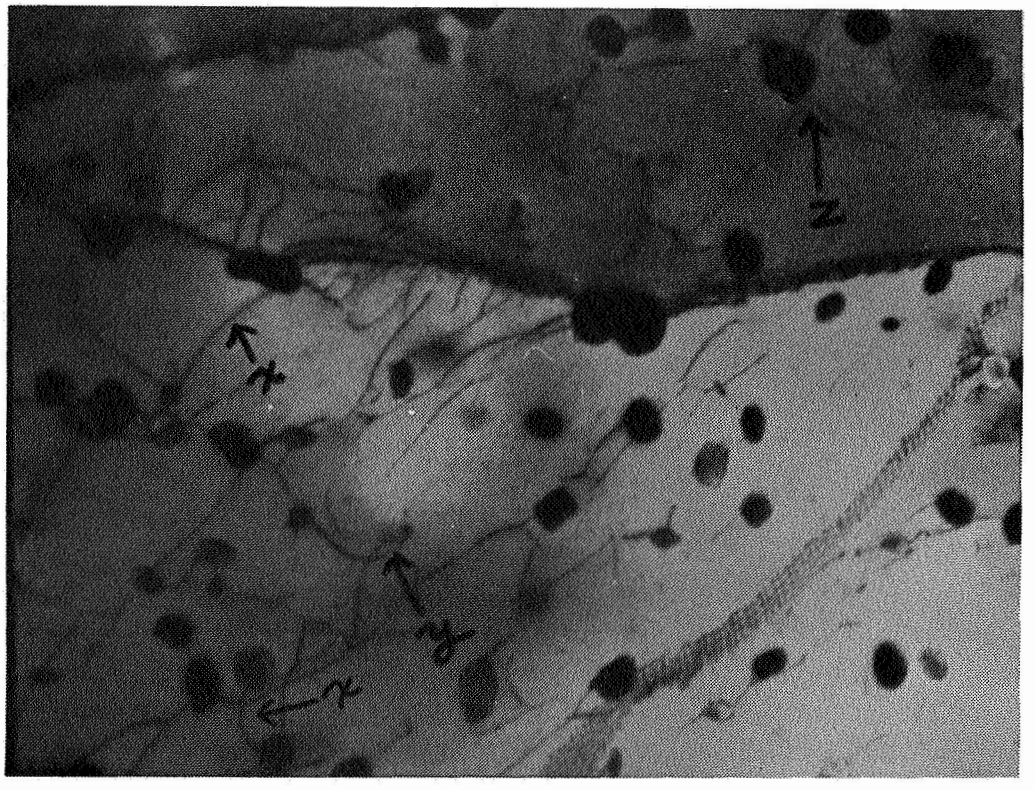

B. Dup D

FIGURE 8. STRUCTURE OF AS-RECEIVED D43 AFTER 9 PERCENT CREEP STRAIN: 32,000 X MAGNIFICATION

there is ample evidence that particles obstruct dislocation movement during creep. Therefore, the rate controlling dislocation mechanism is likely to be one whereby dislocations overcome obstacles by cross-slip or climb.

Screw dislocations should easily bypass particles by cross-slip at the temperature of these tests. The cross-slip of screw dislocations over particles will thus contribute to the observed dislocation structures, but this mechanism is not likely to be rate controlling. Therefore, the rate controlling creep mechanism is likely to be the slower mechanism, i.e., climb of edge dislocations over carbide particles. This postulated mechanism is in agreement with the almost equal values for the activation energy for creep and that for self-diffusion in D43, as discussed in Section 2.1.2. On this basis, the dislocation configurations near particles in Figures 7A and 8 are those resulting from the following: edge dislocations held up by particles and bowing out between them (X in Figures 7B and 8B), dislocations which are partly wrapped around particles where climb is not yet complete (Y in Fig. 8B) and dislocations that have surmounted particles by climb. It has been postulated that the latter mechanism will result in edge dislocations containing climb jogs. This mechanism could account for the wishbone shaped dislocation configurations observed near some of the particles (Z in Figures 8A and B). It should be realized, however, that the above simplified models are likely to be complicated in any real crystal by the interactions of dislocations of mixed edge and screw character with each other and with carbide particles.

2.2 THE EFFECT OF AN INTERSTITIAL SINK ON CREEP BEHAVIOR

In this section data showing the creep behavior of as-processed D43 subjected to titanium sinks and titanium-columbium sinks are presented. The general shapes of the creep curves, the activation energies, the stress dependencies and the structures are analyzed to determine the effects of interstitial sinks on the creep behavior of this alloy. In the first sub-section below,data are presented to show the effect on the creep rate of a titanium sink acting on the specimen during creep testing and of a titanium sink applied to the specimens before creep testing. For the former tests, the specimens were creep tested with the titanium sink diffusion bonded to their surfaces. For the latter tests, the specimens were heated (2200° F for 57 hours) with an interstitial sink diffusion bonded to their surfaces and then the sink was removed before creep testing the specimens. It has been shown in the First Interim Report that this precreep heat treatment will drastically reduce the interstitial concentration and thus the amount of the dispersed phase in the D43. The creep behavior of these sink treated specimens is compared with the creep behavior of both the as-processed alloy and the alloy given the same precreep heat treatment without an interstitial sink. In the remaining subsections, data are presented to show the effect on the creep behavior of precreep heat treatments with interstitial sinks of varying chemical potentials. This latter study shows the effect on the creep rate of D43 of interstitial sinks with different affinities for the interstitials in the alloy. In effect, the study reveals the creep rate of D43 with interstitial concentrations reduced to different levels by the various sinks.

2.2.1 The Effect of a Titanium Sink on the Creep Rate of D43

The effect of a titanium sink on the creep rate and the shape of the creep curves are discussed in this section. The cases considered are those where the titanium is effective in removing interstitial from the D43 during creep testing and before creep testing.

The Effect of a Titanium Sink in Place During Creep

The effect of a titanium sink in contact with the specimen during creep testing on the creep behavior is shown in Fig. 9. For this test the strength of the titanium has been neglected, since its strength at 2200° F is only ~200 psi and it constitutes only 10 percent of the specimen cross-section. A comparison of the two curves shows the effect of the progressive removal of carbon on the creep rate of D43 (Dup D). The creep rate increases continuously, and the creep life of the alloy is drastically shortened by the action of the titanium sink during creep testing. The titanium sink induces an almost immediate increase in creep rate of the alloy relative to the as-received alloy not subjected to a titanium sink. The creep rate of the specimen tested with titanium initially increases and then attains a steady state creep rate at a strain greater than ~3 percent. The greatest increase in the creep rate caused by the action of the titanium sink occurs within the first 150 minutes of the test. As previously shown, this is also the period of time when the greatest amount of carbon (and, therefore, carbides) is removed from the alloy. The carbon in D43 subjected to a titanium sink is reduced to about half of its initial value during the first 100 to 200 minutes at 2200° F while some 3000 minutes are required for most of the remaining carbon to be removed. Since the creep rate of the alloy is determined by its structure (for the conditions of constant stress and temperatures used in these tests) the greatest changes in structure must also occur during this initial period of increasing creep rate and maximum carbon (carbide) removal. These results show the marked effect of the carbon concentration on the creep rate and, therefore, on the structure of D43. Clearly, carbide removal (by a titanium sink) during creep tests changes the structure and increases creep rate of this alloy.

Titanium Sink Effective Before Creep

The effects on the creep behavior of annealing the differently processed D43 alloys with and without a titanium sink are shown in Figures 10-12. Creep specimens were heat-treated for 57 hours at 2200° F prior to creep testing. This heat treatment significantly decreases the creep life of this alloy. However, the reduction in creep life is much more severe for specimens annealed with the sink than for those similarly annealed without the sink. The action of the sink in removing the carbide particles reduces the alloy to one that is solution strengthened rather than dispersion strengthened.

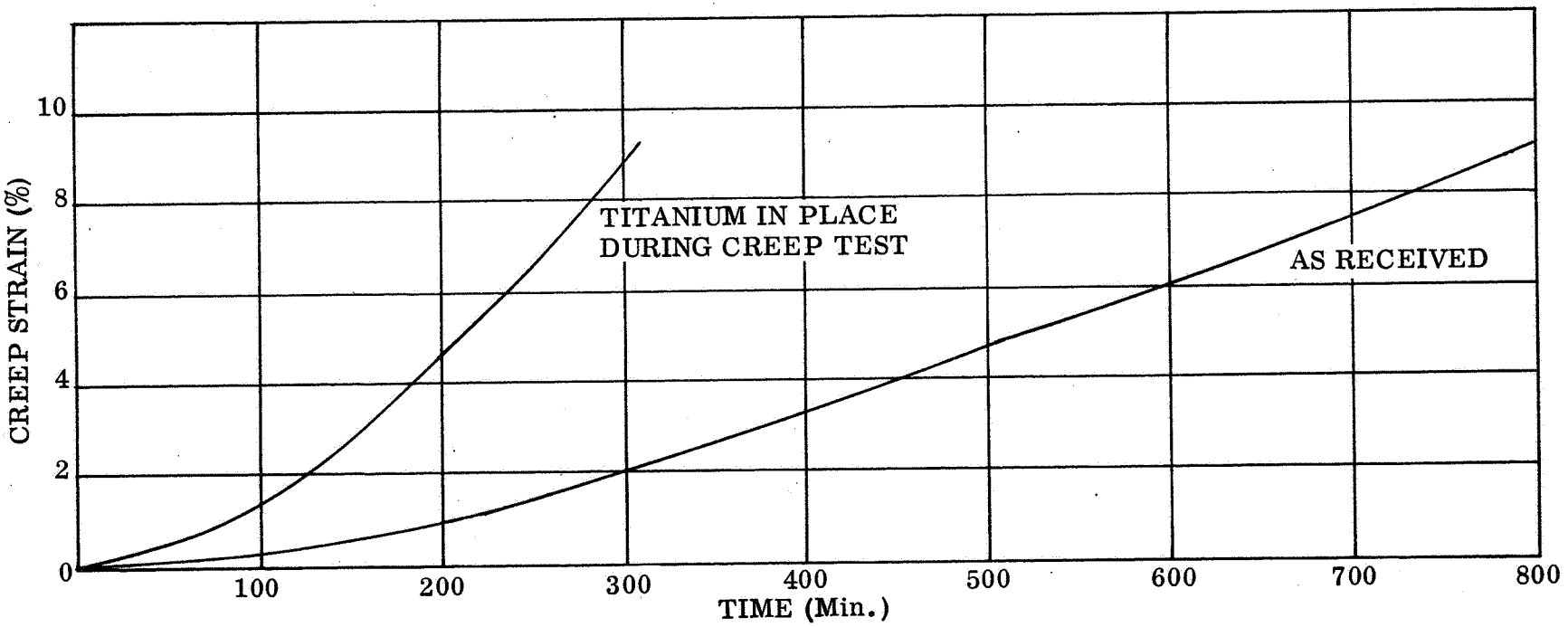

FIGURE 9. THE EFFECT OF A TITANIUM SINK IN PLACE DURING CREEP TEST ON THE CREEP BEHAVIOR OF D43 (DUP D) AT 2200 F (15,000 PSI)

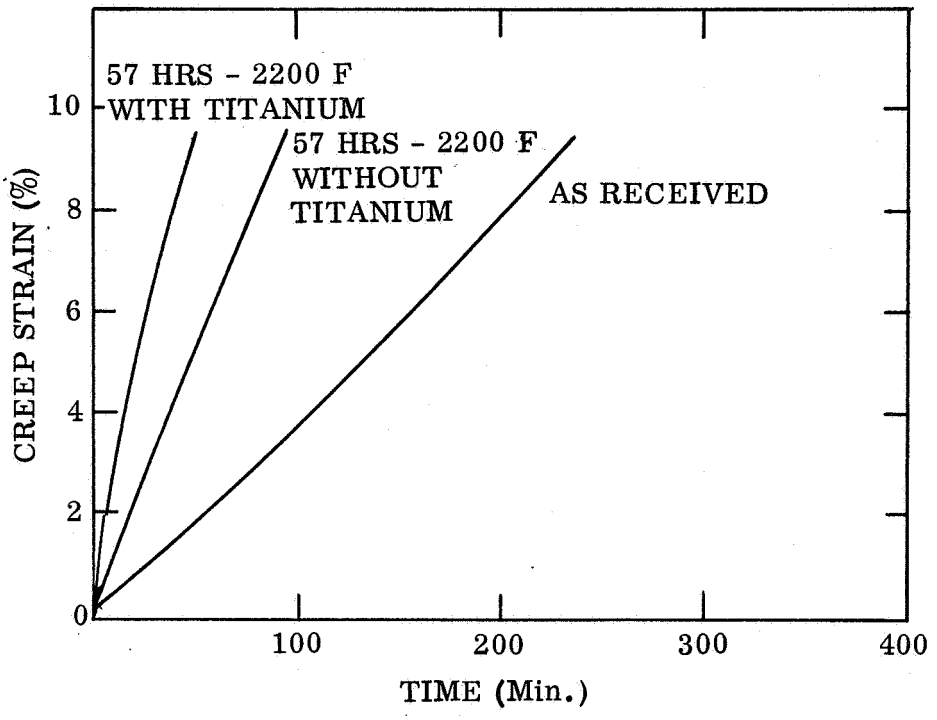

FIGURE 10. THE EFFECT OF A TITANIUM SINK ON THE CREEP BEHAVIOR OF D43 (DUP F) AT 2200 F (15, 000 PSI)

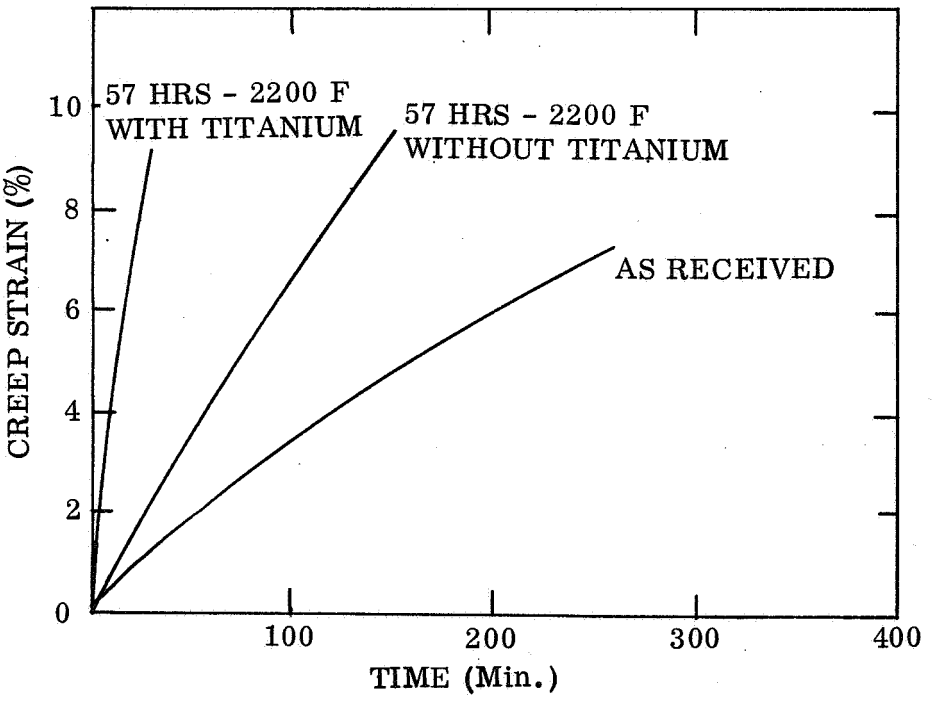

FIGURE 11. THE EFFECT OF A TITANIUM SINK ON THE CREEP BEHAVIOR OF D43 (STD. F) AT 2200 F (15, 000 PSI)

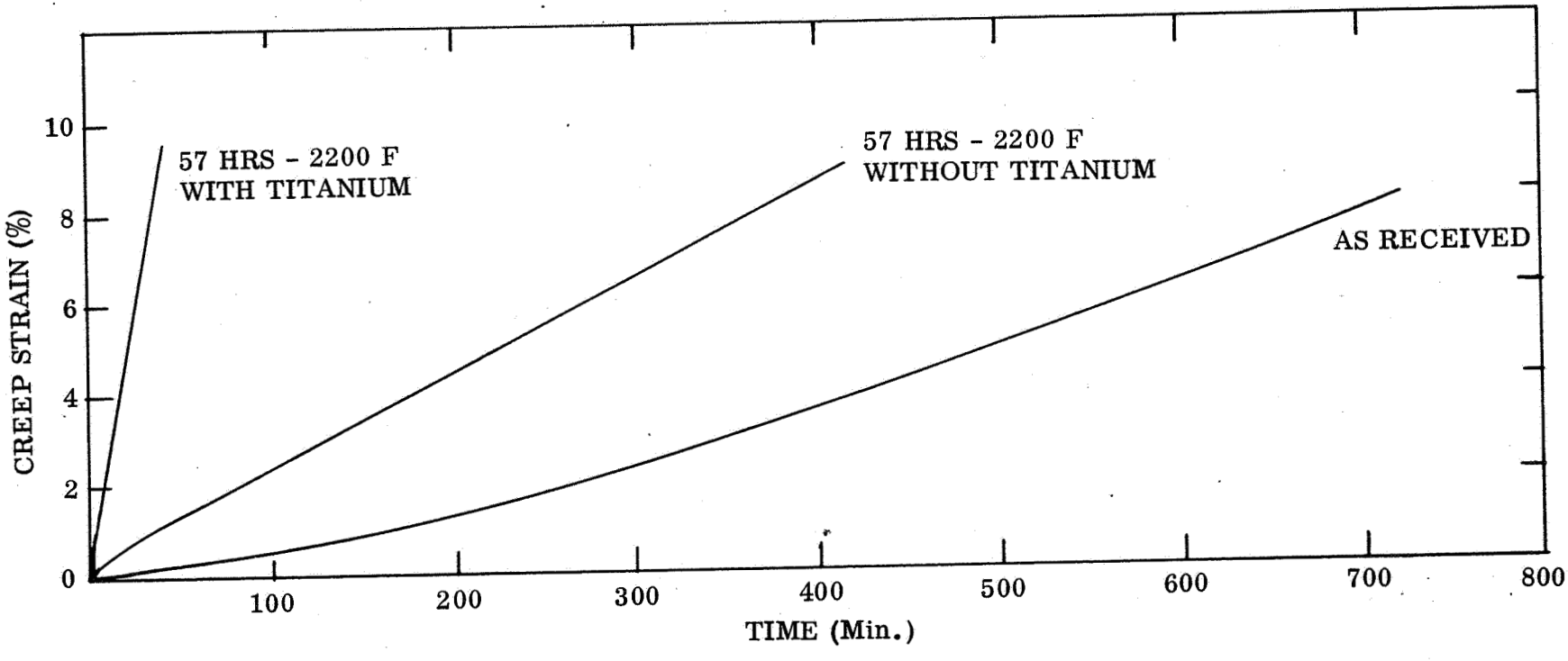

FIGURE 12. THE EFFECT OF A TITANIUM SINK ON THE CREEP BEHAVIOR OF D-43 (DUP. D) AT 2200° F (15,000 psi)

It is evident that the carbide dispersion is an essential factor enhancing the creep life of this alloy since its removal reduces the creep life of the differently processed material to about the same low level. In effect, the processing condition of the alloy is erased by the action of the sink. However, the effect of processing is still evident for specimens annealed without a sink since the creep life of Dup D is still much greater than those of Dup F and Std F after this annealing treatment.

2.2.2 The Effect of Sink Composition on Creep Rate

In this section work performed during the previous period concerning the partition of carbon between a series of Cb/Ti foils and D43 will be briefly reviewed to provide a background for a continuation of this work this period. The actual equilibrium partition of carbon between the D43 and the interstitial sinks are compared with those calculated from thermodynamic considerations. In addition, the effect of the different interstitial sinks on the creep rate of D43 are discussed in terms of the reductions of the carbide phase in the alloy by the various sinks.

Thermodynamic Considerations

The equilibrium partition of interstitials between a refractory metal and a sink metal (foil) is determined by the difference in the partial molar free energy (μ) of the interstitials in the two metals. As previously discussed, μ can be varied by changing the composition of the interstitial sink since

$$\mu = \Delta F^{\circ} + RT \ln C/S. \qquad (10)$$

In this equation μ is the change in free energy (partial molar free energy or chemical potential) of the interstitial in solution in the sink alloy foil, ΔF° is the free energy of formation of the interstitial compound), C is the concentration of interstitial in solution in the alloy, T is the temperature, and S is its saturation solubility. The two terms affecting μ (and thus the partition of interstitials between the alloy foils and the refractory metal) at a constant temperature are ΔF° and S.

Using this equation, the equilibrium partition of carbon between a series of Ti-Cb interstitial sink foils and columbium was calculated and the results were presented in the previous report. The calculated values were compared with the experimental data for the partition of carbon between the alloy sink foils and D43. Comparisons were made between calculated values and experimental values using the initial compositions of the alloy foils rather than those after the alloy foil/D43 diffusion couples had been annealed at 2200°F. For these calculations, it is assumed that the composition of the sink foils and the columbium (D43) remain constant while the carbon assumes an equilibrium partition between them. In effect, the composition (chemical potential) of the interstitial sink is taken to be constant during the time required for carbon to concentrate in the sink. However, as described in the previous report, the composition (chemical potential) of titanium in the foils is reduced by dilution with columbium from the D43.

During this period the compositions of the alloy foils was determined by electron microprobe analyses after the diffusion couples were annealed at 2200° F for 57 hours. A comparison was made of the partitions of carbon in the alloy foil/D43 couples for the annealed foil compositions (rather than the initial foil compositions). The changes in foil composition induced by annealing are shown in Table III (for 0.0045 inch foils on 0.020 inch D43). Compositional changes in the foil are greatest for alloy foil/D43 diffusion couples where the alloy foil is high in titanium. As previously discussed, dilution of the foils with columbium is severe for the Ti/D43 system because of the high intrinsic diffusion of titanium relative to columbium. The calculated and experimental carbon concentration remaining in the D43 are shown in Fig. 13 for both the initial and final foil compositions. The calculated percentages for carbon remaining in columbium at equilibrium partitions are in reasonable agreement with the experimental values for carbon remaining in the D43.

Variations in Creep Rate with Sink Composition

The D43 specimens whose carbon concentrations are shown in Fig. 13 were tested in creep after they had been annealed at 2200° F in contact with the various alloy foils. As previously described, the alloy foil and the diffusion zone were removed from the creep specimens before measuring their creep life. The creep data (labeled according to the initial composition of the alloy foils) are shown in Fig. 14. It is evident that the creep life of D43 is a sensitive function of the composition (chemical potential) of the interstitial sink to which it is subjected. A sink containing ten atomic percent titanium in columbium (Ti-90Cb) is sufficiently active to significantly reduce the creep life of D43.

For the conditions of these tests (constant stress and temperature) the creep rate will be a function only of the metal structure. Thus, a more significant factor than the composition of the sink in considering the creep behavior of these specimens is

TABLE III

CHANGES IN THE ALLOY FOIL COMPOSITIONS INDUCED BY ANNEALING THE ALLOY FOIL/D43 COUPLES FOR 57 HOURS AT 2200° F

	FOIL COMPOSITION ATOMIC PERCENT					
Before Annealing	Ti	Ti-30Cb	Ti-60Cb	Ti-90Cb	Ti-99Cb	Cb
After Annealing	Ti-22Cb	Ti-51Cb	Ti-69Cb	Ti-90Cb	Ti-99Cb	Cb

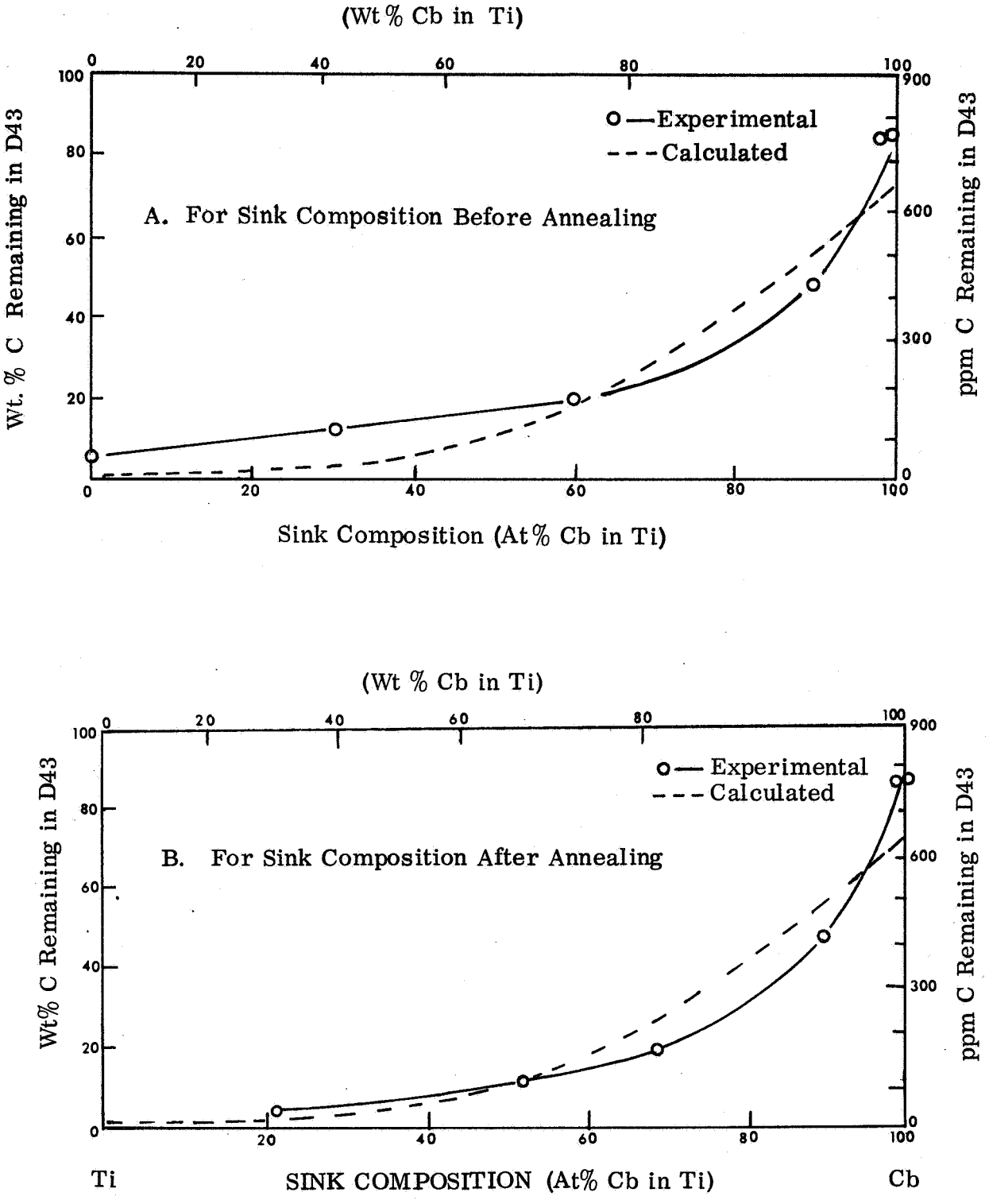

FIGURE 13. CARBON REMAINING IN D43 AFTER EQUILIBRIUM PARTITION AT 2200 F AS A FUNCTION OF THE COMPOSITION OF THE INTERSTITIAL SINK.

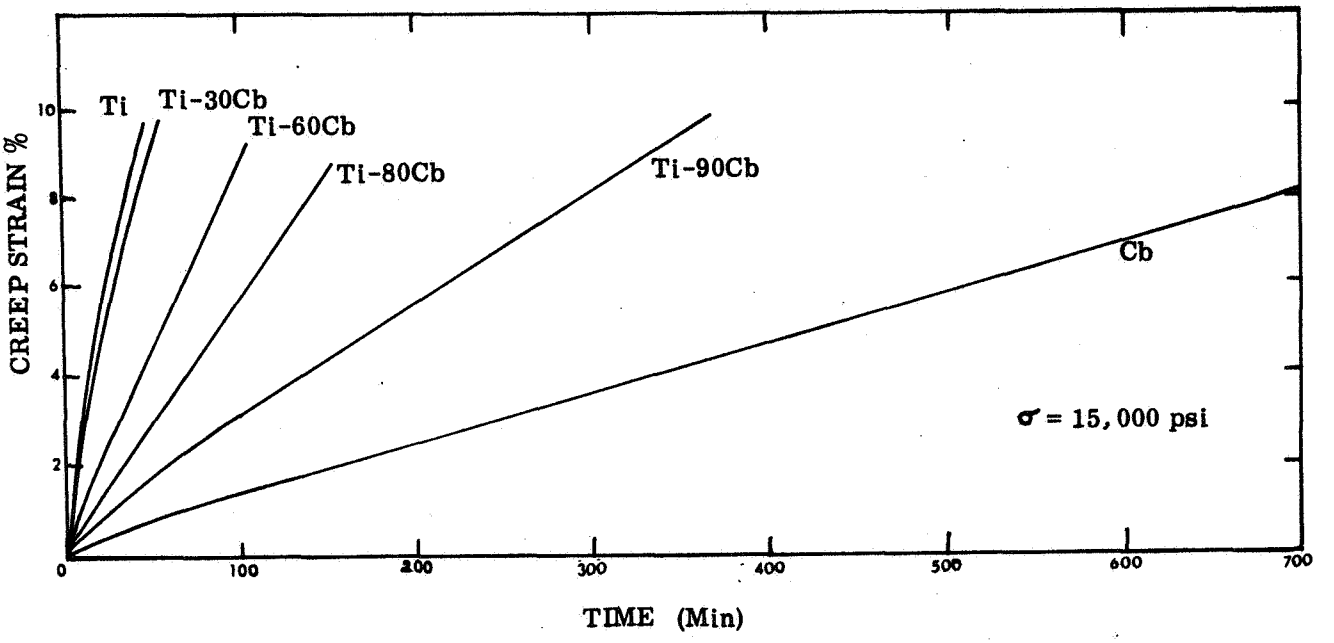

FIGURE 14. EFFECT OF THE COMPOSITION OF THE INTERSTITIAL SINK ON THE CREEP RATE OF D43 AT 2200 F. THE INITIAL INTERSTITIAL SINK COMPOSITIONS ARE SHOWN BY EACH CREEP CURVE

their carbon concentration since this is a measure of the amount of carbides in their structure. Previous work has shown that carbon is the major interstitial in D43 and that carbon can be used as a measure of the amount of interstitial precipitates (complex carbides or oxides) remaining in this alloy to strengthen it. For convenience in the following discussion, the interstitial phases contributing to the high temperature strength of D43 through their influence on structure will simply be referred to as a carbide. In Fig. 15A the steady state creep rates derived from the data of Fig. 14 are shown as a function of the carbon concentrations in the specimens. These results show that the creep rate is a sensitive function of the carbon concentration and thus the amount of carbides in this alloy.

For a creep rate, $\dot{\epsilon}^{\circ}$, controlled by the climb of edge dislocations over particles the creep rate can be defined as (Ref. 4)

$$\dot{\epsilon}^{\circ} = NAb\ R \tag{11}$$

where N is the number of particles per unit volume, A is the area swept out by a dislocation after climbing over an obstacle, b is the Burgers vector and R is the climb rate. For this physical situation it can be shown that

$$\dot{\epsilon}^{\circ}\ a\ \frac{r}{f} \tag{12}$$

where r is the particle radius and f is the volume fraction of second phase particles.

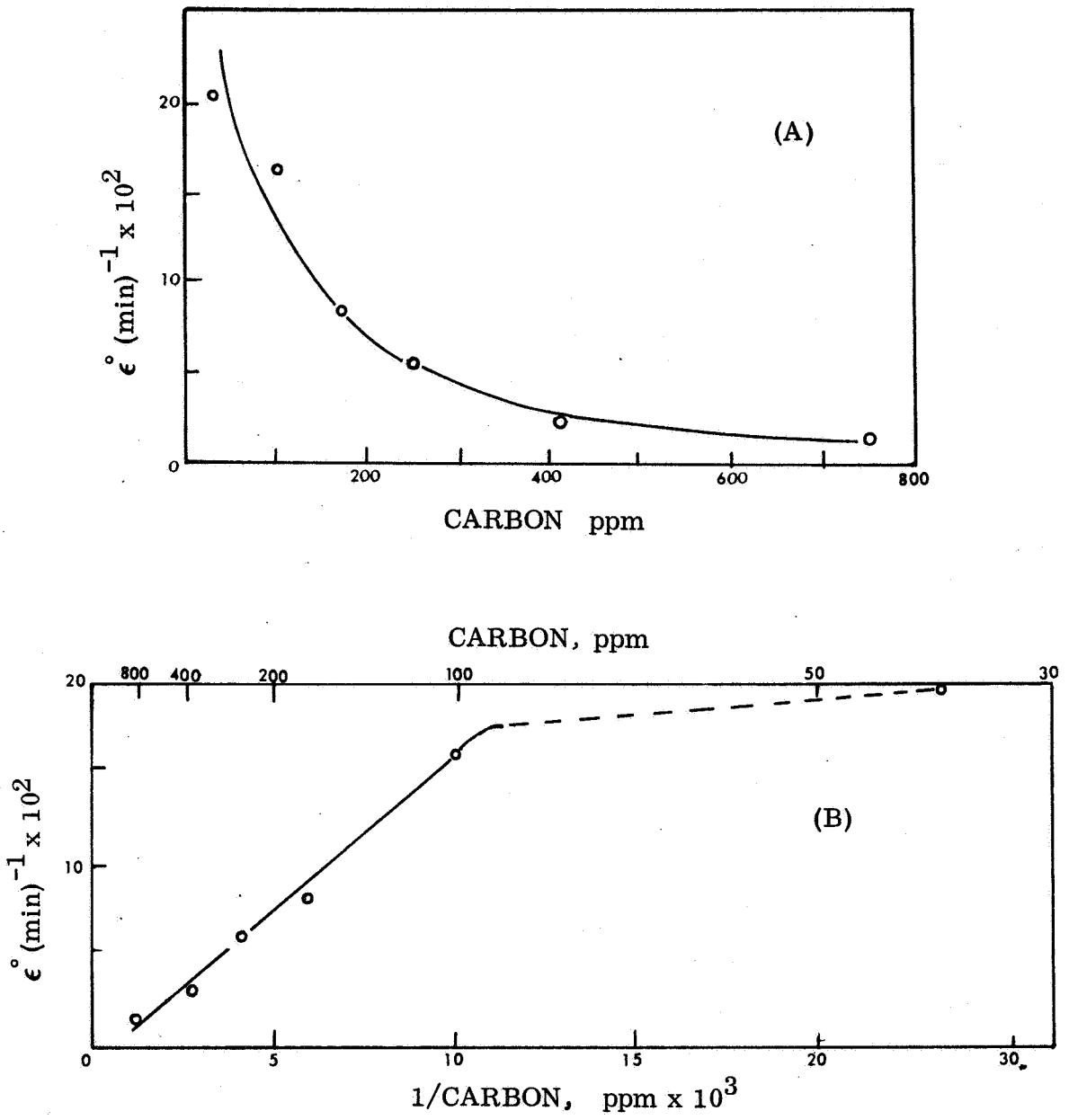

FIGURE 15. STRAIN RATE AS A FUNCTION OF THE CARBON CONCENTRATION IN D43.

Since the weight fraction of carbon, C, is a to the volume fraction of carbide in D43, ϵ° should be linear with $(C)^{-1}$ if the particle radius remains approximately constant while the interparticle spacing varies. The data plotted in Fig. 15B show that the creep rate is inversely proportional to the carbon concentration to 100 ppm carbon. The approximate linear relationship derived from these data is

$$\epsilon^{\circ} = 1.7 \times 10^{-2} C^{-1}. \tag{13}$$

For carbon concentrations below 100 ppm the creep rate and hence the structure is relatively independent of the carbon concentration. For carbon concentrations less than 100 ppm the carbon is likely to be for the most part in solution at 2200° F so that the structure and hence the creep rate will be independent of the carbon concentration. The relationships between the carbon concentration and the creep life of D43 indicated by these results can be summarized as follows:

For $C < \sim 800$ and > 100 ppm the distribution and volume fraction of carbides control the creep rate through their influence on structure so that

$$\epsilon^{\circ} = f(S)_{\sigma T} = \phi(C)_{\sigma T}$$

For $C < 100$ ppm the creep rate is a function of structure independent of the carbon concentration so that

$$\epsilon^{\circ} = f(S)_{\sigma T} \neq \phi(C)_{\sigma T}$$

where S is the structure, and σ is the stress.

2.2.3 The Effect of a Sink on the Activation Energy for Creep

The activation energies for creep for specimens tested at 2200° F are listed in Table IV as a function of strain for the following conditions: the as-processed alloy; the as-processed alloy after a precreep heat treatment of 57 hours at 2200° F, the as-processed alloy after a precreep heat treatment of 57 hours at 2200° F with a titanium sink. Although the activation energies are relatively constant with strain, within the scatter in experimental determinations, there is some tendency to higher values at low strains (e.g., 2200° F 57 hrs with Ti in Table IV). As previously discussed, the activation energies for the as-processed Dup D are, in general, lower than those for the as-processed Std F and Dup F. The average value of the activation energy of 96 K cal/mole for Dup D in the as-processed condition lies just outside the range of values determined by comparing the standard deviation (10) with average of the other activation energy values (115) in Table IV. However, heating the Dup D material either with or without a titanium sink results in an increase in the activation energy to an average value near those for the Std F and Dup F conditions. As previously

TABLE IV

ACTIVATION ENERGIES FOR CREEP OF D43 AT 2200° F

Creep Strain(%)	ACTIVATION ENERGIES x 10^{-3} Cal/Mole								
	As-Processed			2200° F/57 Hrs. No Ti			2200° F/57 Hrs with Ti		
	Std F	Dup F	Dup D	Std F	Dup F	Dup D	Std F	Dup F	Dup D
0.8	136	126	82	135	113	121	146	135	124
1.6	131	125	91	123	128	110	137	126	132
2.4	97	123	110	117	113	106	113	110	122
3.2	120	120	94	111	105	102	109	103	108
4.0	128	111	98	124	124	110	124	131	107
5.8	112	127	99	110	108	104	99	100	102
6.6	101	112	89	99	101	100	109	126	117
7.3	113	108	102	106	111	102	104	107	111
8.2	102	115	107	118	120	122	117	102	126
9.0	121	110	95	108	99	110	107	125	105
Averages	116	118	96	115	112	110	117	117	115

discussed, (Sec. 2.1.2) this difference in activation energy for the as-processed Dup D may be caused by a difference in the partition of a substitutional element between the matrix and the precipitate. It is interesting to note that heat treating the alloy for 57 hours at 2200° F does not significantly change the average activation energies for the Std F and Dup F conditions even though this heat treatment drastically reduces the density of dislocations and subgrains in the alloy. In addition, the almost complete removal of the interstitial phase prior to creep by the action of the titanium sink does not induce a significant change in the activation energy relative to those for the alloy heat treated without a sink. Table V lists the activation energies for D43 (Dup D) heated without a sink and with progressively stronger sinks. It is evident that the progressive reduction of carbon (carbides) by the sinks does not significantly change the activation energy for creep of this alloy. These results show that the activation energy for creep is not much affected by the dislocation or second-phase structures in D43.

2.2.4 The Effect of an Interstitial Sink on the Stress Dependence of the Creep Rates

The stress dependences of the creep rates were determined for a series of D43 (Dup D) specimens that had been exposed to interstitial sinks with compositions ranging from unalloyed columbium to unalloyed titanium. As previously discussed in Sec. 2.2.2, this precreep sink treatment (2200° F / 57 hrs) reduces the carbon

TABLE V

THE EFFECT OF INTERSTITIAL SINKS ON THE ACTIVATION ENERGY FOR CREEP OF D43 (DUP D) AT 2200° F

	SPECIMEN TREATMENT				
		2200° F/57 Hrs with the Sink Compositions Listed Below			
	As-Processed	No Sink	Ti-90Cb Sink	Ti-60Cb Sink	Ti Sink
No.of Determinations	10	10	5	10	10
Ave. ΔH Value (Cal/Mole x 10^{-3})	96	110	108	114	115

concentration of the specimens to levels proportional to the concentration of titanium in the sink. The stress dependencies of the creep rates at 2200° F are shown in Fig.16 labeled according to the composition of the sink foils to which the specimens were exposed. The slopes of the log strain rate versus stress plots are seen to be about the same over the range of stress tested. As shown in Table VI, a reduction in the carbon concentration by exposure of the specimens to the various sinks does not significantly change the stress exponent from that for the as-processed alloy.

TABLE VI

STRESS EXPONENT, n, FOR D43 (DUP D) EXPOSED TO INTERSTITIAL SINKS OF DIFFERENT COMPOSITIONS

	SPECIMEN TREATMENT					
		2200° F/57 Hrs with the Compositions Listed Below				
	As-Processed	Cb	Ti-90Cb	Ti-60Cb	Ti-30Cb	Ti
Stress Exponent, n ($\epsilon^{\circ} \alpha \sigma^{n}$)	7.7	8.0	8.3	7.9	7.7	7.9

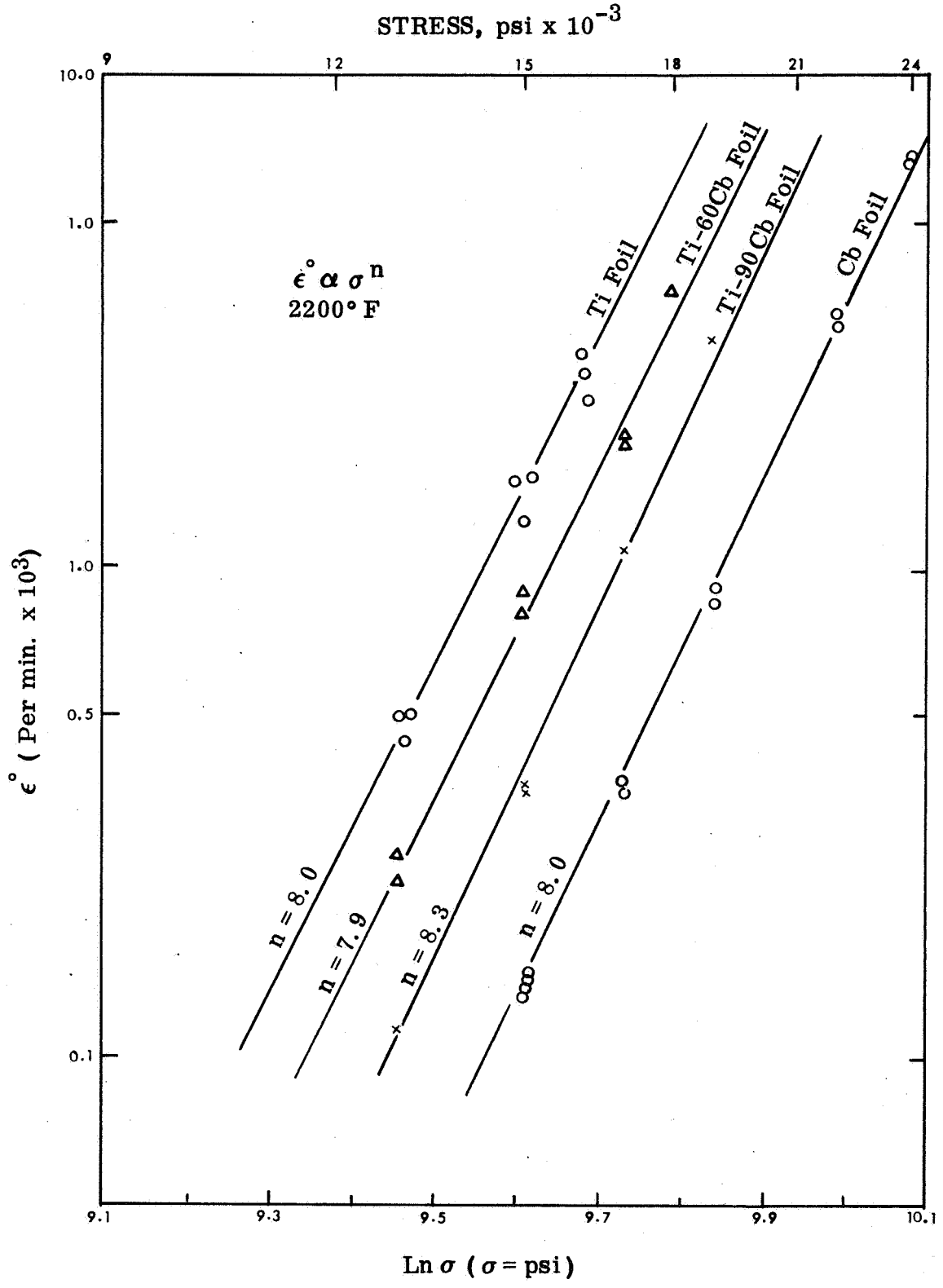

FIGURE 16. THE EFFECT OF STRESS ON THE STEADY-STATE CREEP RATE OF D43 (DUP D) EXPOSED TO INTERSTITIAL SINK FOILS OF DIFFERENT COMPOSITION

2.2.5 The Relationship Between the Structure, the Creep Rate and the Sink Composition

Fig. 17 shows the effect of heat treatments without and with a titanium sink on the structure of D43 (Dup D). As previously discussed, the as-processed alloy is inhomogeneous with respect to the size and distribution of the subgrains and carbide particles. Nevertheless, the 57-hour heat treatment at 2200°F without a titanium sink has rendered the specimen almost devoid of its initial substructure without evident loss of the carbide particles (Fig. 17B). It is difficult to determine if the heat treatment has altered the average carbide distribution or size because of the large variation in sizes and distributions observed. However, the reduced creep life induced by this heat treatment (Fig. 12) suggests that some agglomeration of carbide particles may have taken place as a result of this heat treatment. As previously discussed, the obstructions offered to dislocation movement by carbides contribute significantly to the creep life of this alloy. The effect of a titanium sink on the structure of D43 is shown in Fig. 17C. The carbides are removed from the structure by the action of the titanium. This change in structure correlates with a drastic reduction in the creep life of this alloy (Fig. 12).

Fig. 18 shows the structures in the gage sections of D43 (Dup D) specimens after creep strains of about 9 percent at 2200°F. Each of the structures shown are for creep specimens given precreep heat treatments with different interstitial sinks. The composition of the sinks ranged from unalloyed columbium to unalloyed titanium as indicated in Fig. 18. The transmission photomicrographs thus show the creep structures in D43 with carbon concentrations ranging from ~800 ppm (Cb sink) to <50 ppm (Ti sink). The carbon concentrations in these specimens are shown as a function of the sink composition in Fig. 13. It is evident that a decrease in the carbon concentration induced by the action of the interstitial sinks correlate quantitatively with a decrease in the amount of second phase particles in the D43 structures. Further, the volume fraction of particles decreases as the concentration of titanium in the sink increases. The number of carbide particles is not noticeably reduced by annealing the specimens with a columbium sink. From thermodynamic considerations columbium would not be expected to act as an interstitial sink for D43. However, even the weak (low chemical potential) sinks, Ti-90Cb and Ti-80Cb, noticeably decrease the number of carbides. No carbides were detected in specimens annealed with the stronger sinks Ti and Ti-30Cb and only one region of the specimen annealed with the Ti-60Cb sink was found to contain carbides. Qualitatively, the size of the carbide particles does not appear to change significantly in these specimens; rather it is the number of particles and, therefore, the interparticle spacing that undergoes the greatest change.

As previously pointed out in the discussion of Fig. 17, the structure of D43 given a precreep heat treatment at 2200°F is devoid of substructure and has a low dislocation density. Therefore, the greater dislocation density and the substructure detected in the sink treated specimens after creep (Fig. 18) must have been generated

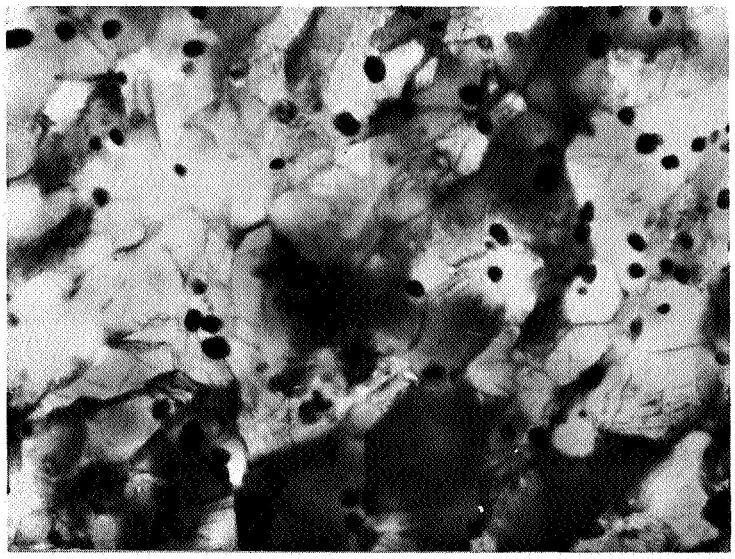

A. As-Processed

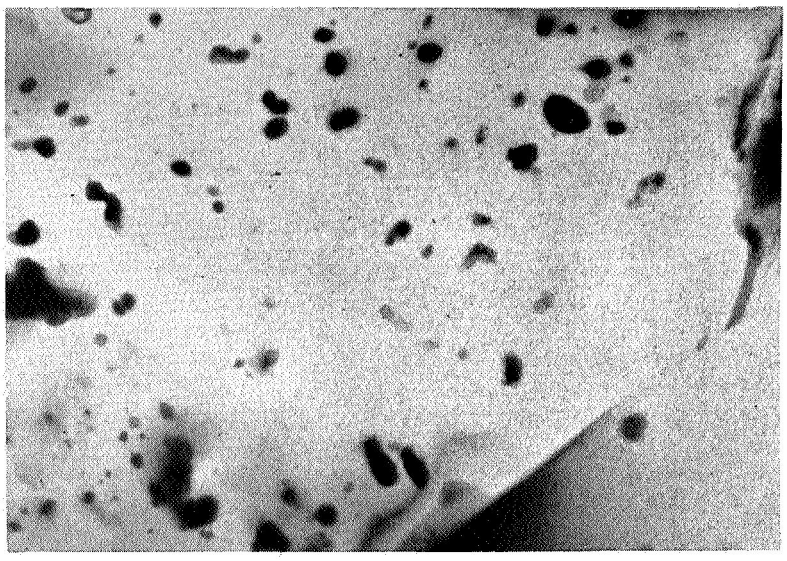

B. Annealed Without a Titanium Sink

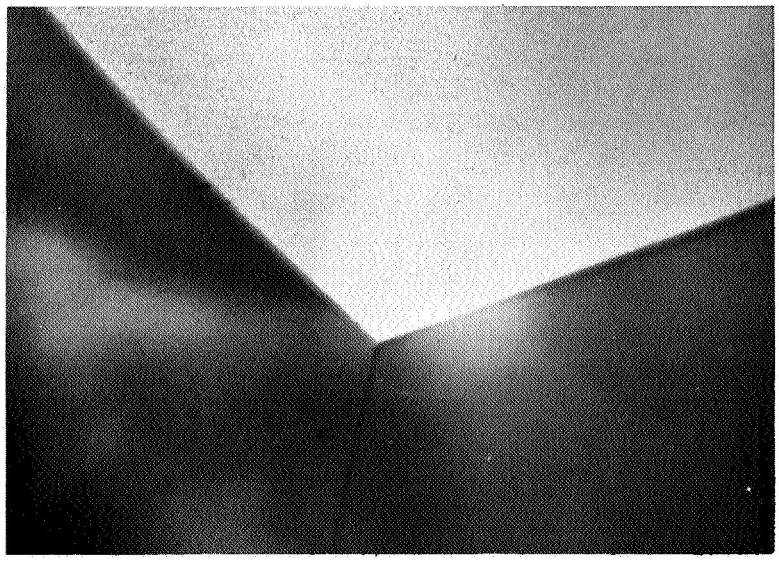

C. Annealed With a Titanium Sink

FIGURE 17. THE EFFECT ON THE STRUCTURE OF ANNEALING AS-PROCESSED D43 (DUP D) WITH A TITANIUM SINK AND WITHOUT A TITANIUM SINK. (Specimens Annealed 57 Hrs at 2200° F: 14,500X Magnification)

A

Cb Sink

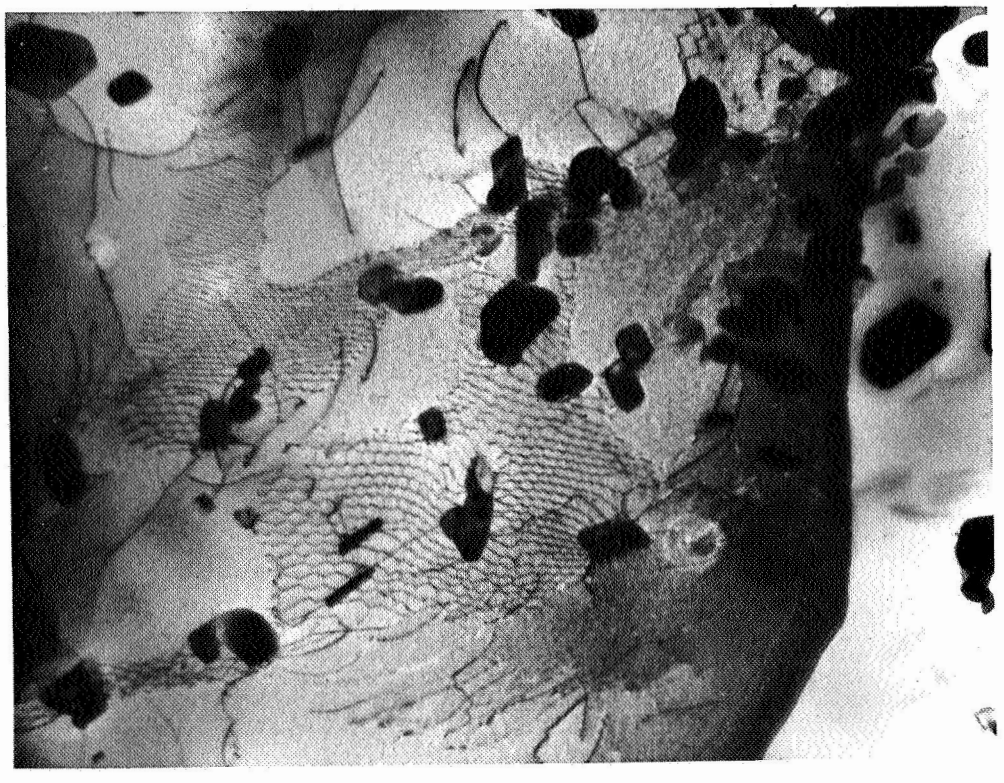

B

Ti/90Cb Sink

FIGURE 18. STRUCTURE OF D43 (DUP D) AFTER 9 PERCENT CREEP STRAIN AT 2200° F. (The specimens were given precreep heat treatments, 57 Hrs/2200 °F, with the interstitial sinks listed adjacent to the micrographs. 32,000 X Magnification) Sheet 1 of 3

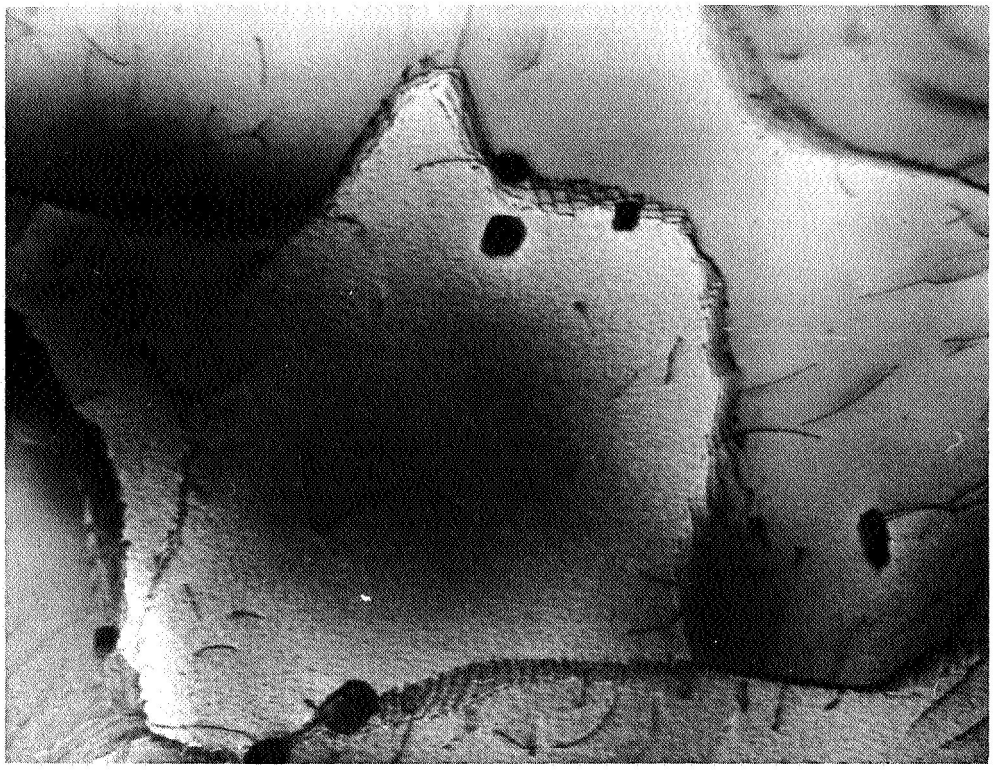

C

Ti/80Cb Sink

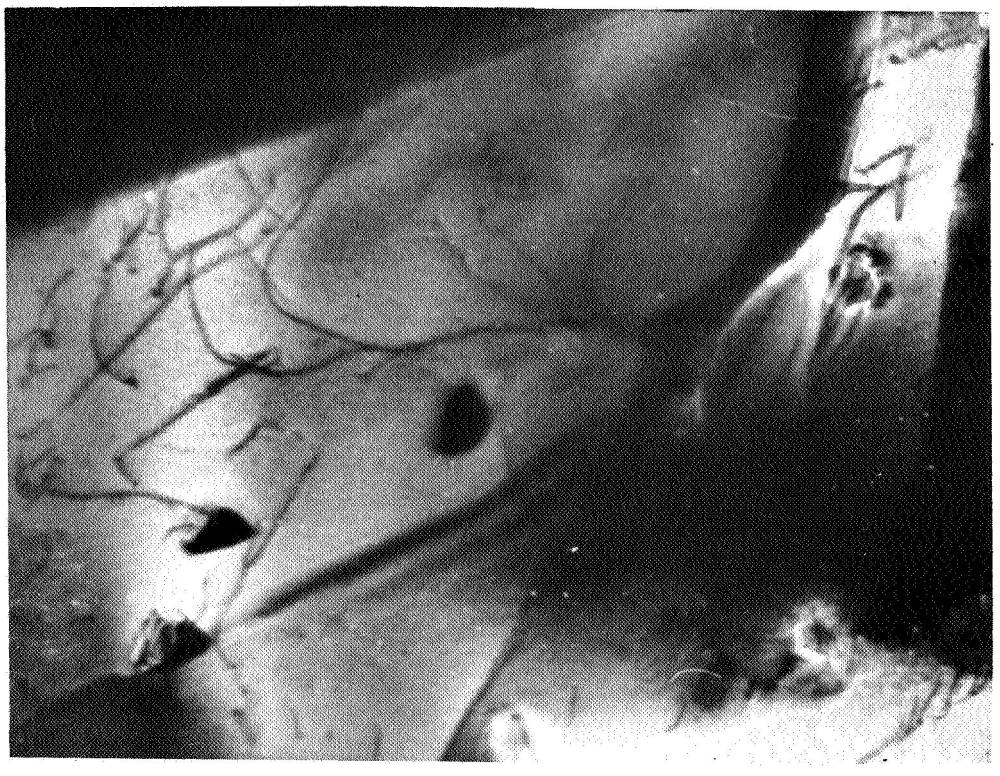

D

Ti/60Cb Sink

FIGURE 18 (Continued - Sheet 2 of 3)

E

Ti/30Cb Sink

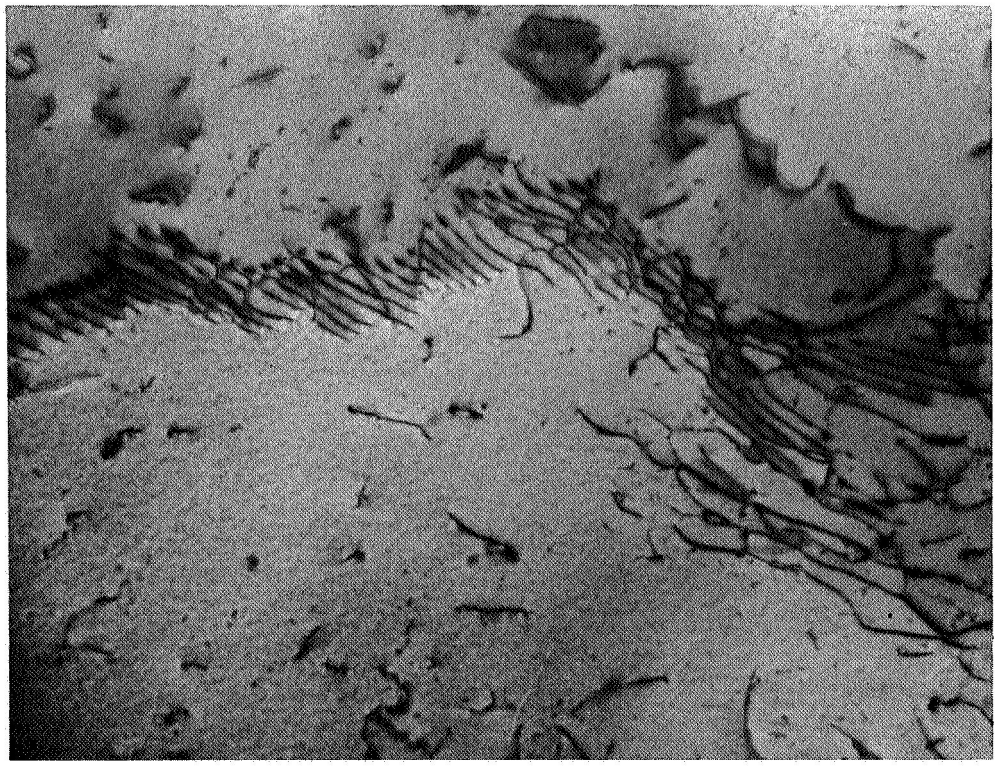

F

Ti Sink

FIGURE 18 (Continued - Sheet 3 of 3)

during creep deformation. The results suggest that the obstructions to dislocation glide offered by the carbide particles tend to increase the uniformity and density of dislocations (Fig. 18, compare A and B with C, D, E and F). In addition, well developed subgrains were observed most often in the specimens that were low in carbides (Fig. 18C and E). Evidently the dislocation interactions required for subgrain formation are retarded by the interactions of dislocations with carbide particles where the density of particles is high.

This investigation has shown that the creep rate of D43 is proportional to the affinity (chemical potential) of the interstitial sink for carbon (Fig. 14). The creep rate is, therefore, also inversely proportional to the carbon concentration remaining in the D43 after exposure to the sink (Fig. 15B). Examination of the structures after creep (Fig. 18) also shows that the creep rate is qualitatively inversely proportional to the number of carbide particles in the alloy. The obstruction offered to dislocation movement by the carbides is evident in Fig. 18A. Here, many instances of dislocation bowing out between carbide particles are evident. The obstructions to dislocation movement are primarily the carbide particles with dislocation networks and other potential obstructions playing a secondary role. The increasing creep rate with decreasing carbon concentration can thus be related directly to the number of carbide particles obstructing dislocation movement. As the carbides are removed from the structure, dislocation networks and subgrains probably become the important structural features controlling the creep rate of this alloy.

III. EFFECT OF TITANIUM ON THE STRUCTURE AND INTERSTITIAL CONCENTRATION OF TZM AND T222

Diffusion couples were prepared by diffusion bonding 0.002 inch titanium or hafnium foil to nominally 0.030 inch T222 and TZM sheet specimens 0.3 inch wide and 2.5 inches long. The bonding conditions used were 15 seconds at 2200° F with a bonding pressure of 8,500 psi. The foils were bonded to both surfaces of flat alloy specimens making Ti/alloy/Ti or Hf/alloy/Hf sandwiches.

All of the diffusion couples were then vacuum annealed to induce interstitial partition to the sinks. The structure and interstitial concentration of part of the specimens were then compared with similarly heat treated specimens that had not been bonded to interstitial sink. The results for the titanium sink are discussed in the first section below: Change in the As-Processed Structures and Interstitial Concentrations Induced by a Titanium Sink.

The remaining T222 and TZM diffusion couples that had been heat treated to induce interstitial partition to the titanium were cold rolled to 75 percent reduction in area and heat treated again at various temperatures to induce recrystallization. These structures were then compared with the structures of specimens that had not been bonded to titanium but had received the same thermal and mechanical treatments. These results are discussed in the second section below: Recrystallization Studies after Annealing with a Titanium Sink Followed by Deformation.

In the third section below the results of some brief studies of the effect of a hafnium interstitial sink on the as-processed structure and the recrystallization of T222 are reported. This system has practical importance in view of the use of Hf-20Ta alloys as claddings and braze alloys.

3.1 CHANGES IN THE AS-PROCESSED STRUCTURES AND INTERSTITIAL CONCENTRATIONS INDUCED BY A TITANIUM SINK

Fig. 19 shows the Ti/alloy structures after diffusion bonding. The structure of the T222 and TZM are those for the as-processed condition and are not influenced by the titanium bonding beyond a narrow diffusion zone. The grains in the TZM are deformed and elongated in the direction of rolling, whereas the grains in the T222 are relatively equiaxed. These grain structures are identical with those in the as-processed but unbonded alloy.

The structures of the as-processed TZM alloy after heat treatments with and without titanium (at 2000° F and 2500° F) are shown in Figures 20 and 21. Heating the TZM (Fig. 20) at 2000° F, both with and without titanium, induces a coarsening of the cold-worked structure without evident recrystallization. After the 2500° F heat

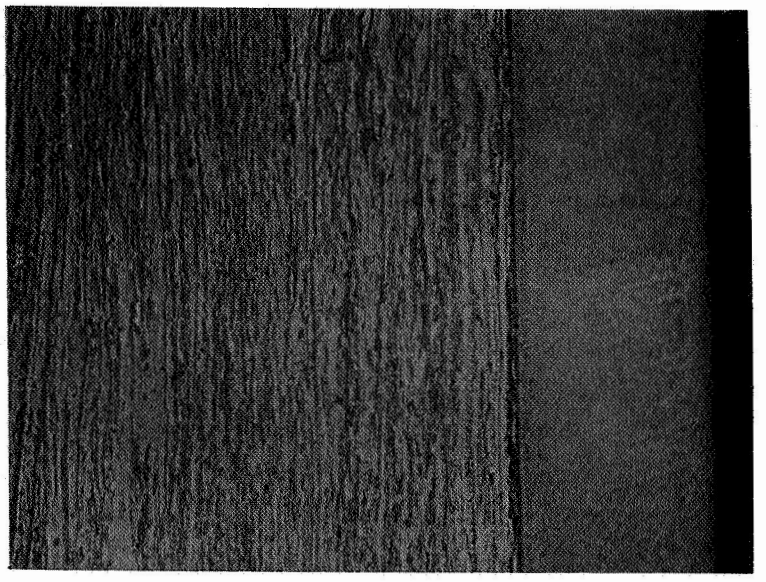

TZM Ti

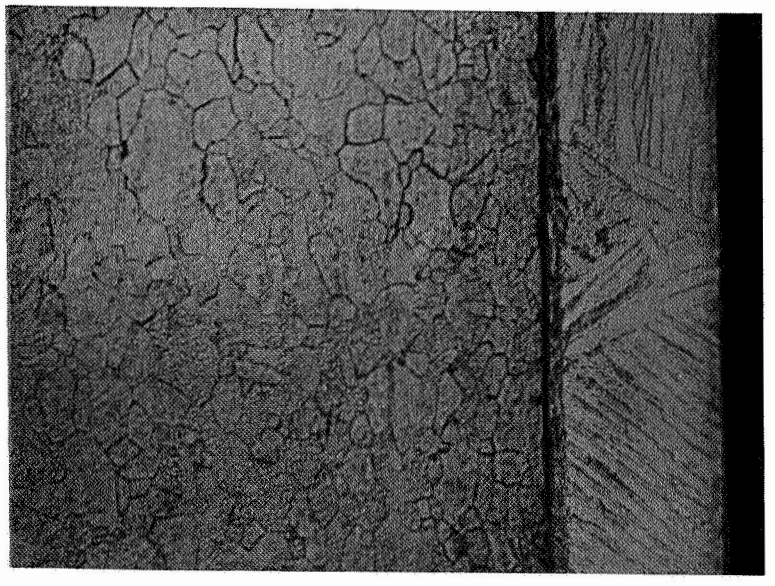

T222 Ti

FIGURE 19. AS BONDED TZM/Ti AND T222/Ti (500X Magnification)

1 Hr/2000 F

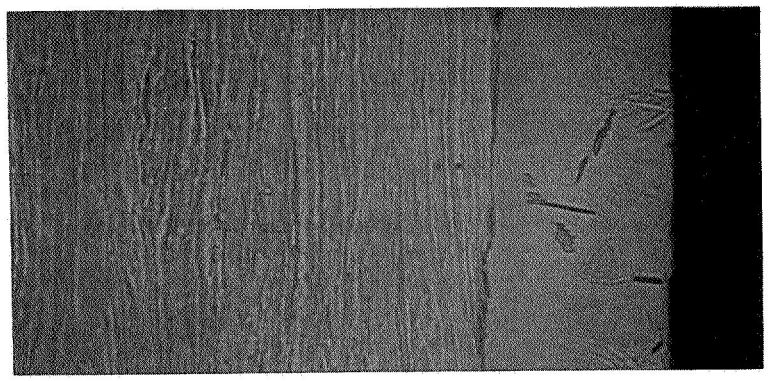

1 Hr/2000 F
Plus Ti

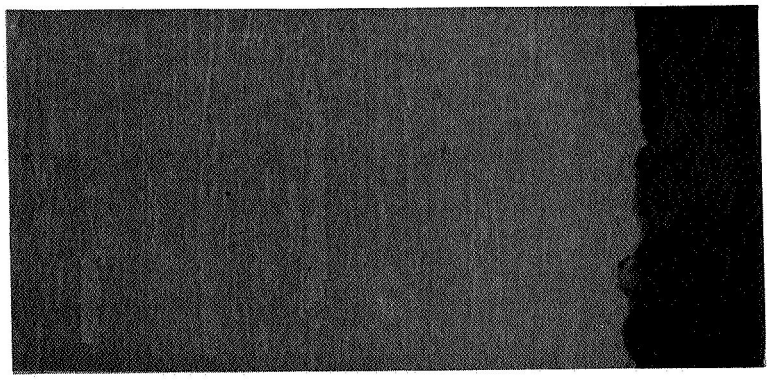

16 Hrs/2000 F

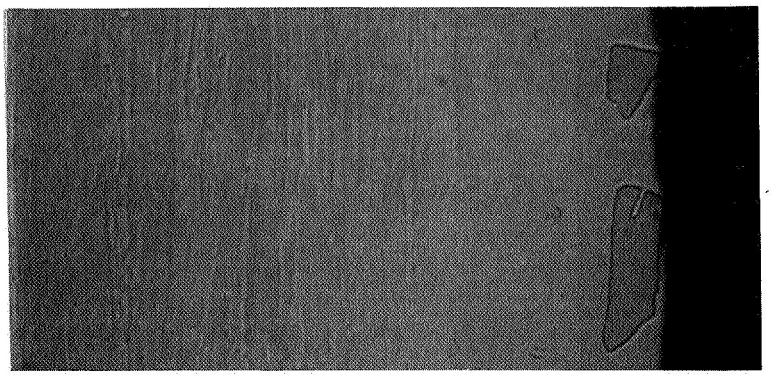

16 Hrs/2000 F
Plus Ti

FIGURE 20. STRUCTURE OF TZM ANNEALED AT 2000° F WITH AND WITHOUT A TITANIUM SINK (500X Magnification)

1 Hr/2500 F

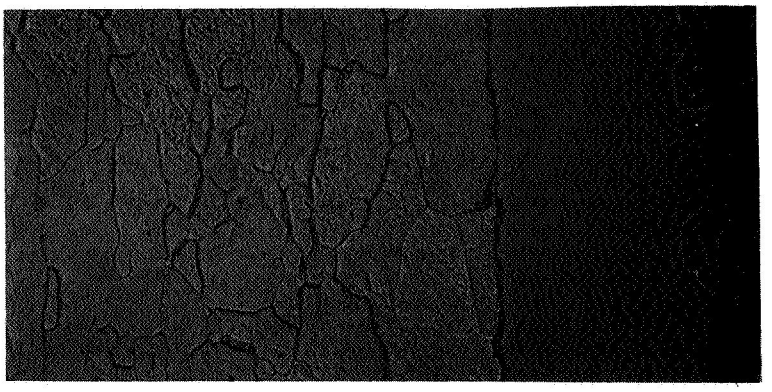

1 Hr/2500 F
Plus Ti

16 Hrs/2500 F

16 Hrs/2500 F
Plus Ti

FIGURE 21. STRUCTURE OF TZM ANNEALED AT 2500° F WITH AND WITHOUT A TITANIUM SINK (500X Magnification)

treatments (Fig. 21) the TZM is fully recrystallized for specimens heated either with or without a titanium sink. However, the grains in the TZM heated with titanium for 16 hours at 2500°F are somewhat more symmetrical than those in the TZM heated without titanium. This series of tests show that titanium, a strong interstitial sink, has a relatively minor effect on the grain structure induced by the recrystallization of the as-received TZM.

As shown in Figures 20 and 21, a second phase is formed in the titanium foil adjacent to the TZM after both the 2000°F and 2500°F heat treatments. This phase is usually found toward the outside of the titanium foils; although in some cases a phase is evident toward the center of the foils. Analysis of one of these particles with an electron probe showed that its composition is approximately that for TiC. This suggests that the titanium is acting as a sink for carbon in the TZM since it will be shown below that the TZM adjacent to the titanium loses carbon.

The structures of the as-received T222 after annealing at 2000 and 2500°F with and without titanium are shown in Figures 22 and 23. The grain structure of the T222 is relatively unchanged by these annealing treatments. The redistribution of interstitials between the alloy and the titanium (if any) is evidently insufficient to alter the grain structure of this alloy. A minor phase is again evident in the titanium after 16 hours at 2000°F and after the 2500°F heat treatments. Carbides were detected with the electron microprobe in the titanium foil adjacent to the T222 heated for 16 hours at 2500°F (Fig. 23). It will be shown below that there is no loss of carbon from the T222 substrate. Therefore, the carbide in the titanium foil may be caused by carbon pick-up during vacuum annealing.

The concentrations of carbon and oxygen in the T222 and TZM after the various annealing treatments with and without titanium are compared in Table VII. The analyses shown as "Plus Ti" are for portions of the heat treated Ti/alloy/Ti diffusion couples analyzed after the titanium had been removed by chemically thinning the couple to 0.026 inch. This center section which is well below the zone of titanium diffusion into the alloys was used as a measure of the effectiveness of the titanium as an interstitial sink for TZM and T222. The nitrogen concentrations were also determined but are not reported here because the concentrations were low (< 10 ppm), and they did not vary significantly with heat treatments. The oxygen concentration in the TZM appears to be slightly reduced by annealing treatments, both with and without a titanium sink (i.e., from ~ 40 ppm to ~ 20 ppm). Although the scatter in analyses is relatively high in this low concentration range, the results are sufficient to show that the titanium used in this study (initial oxygen concentration of ~ 3000 ppm) is not a strong sink for oxygen in TZM. The carbon concentration is significantly reduced by the 2500 and 2700°F annealing treatment, both with and without titanium. In this regard, the vacuum annealing treatments alone appear to be about as effective as the annealing treatment with the titanium sink in removing interstitials from the TZM.

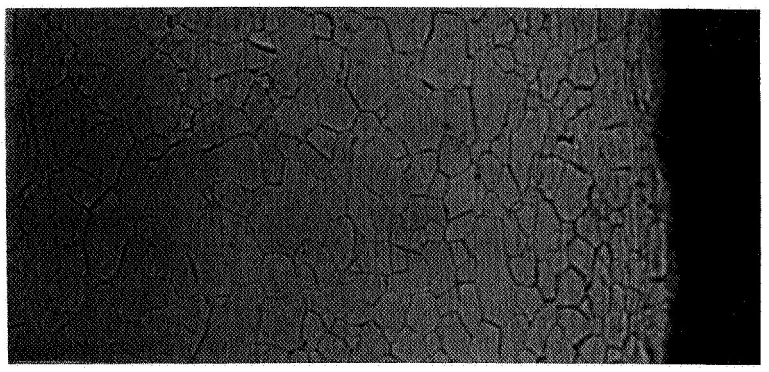

1 Hr/2000 F

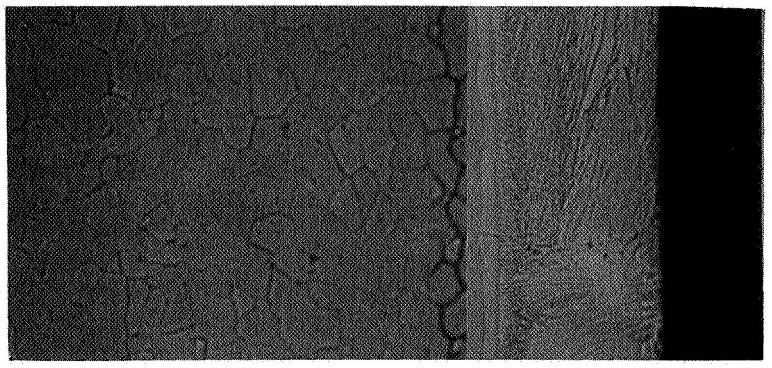

1 Hr/2000 F
Plus Ti

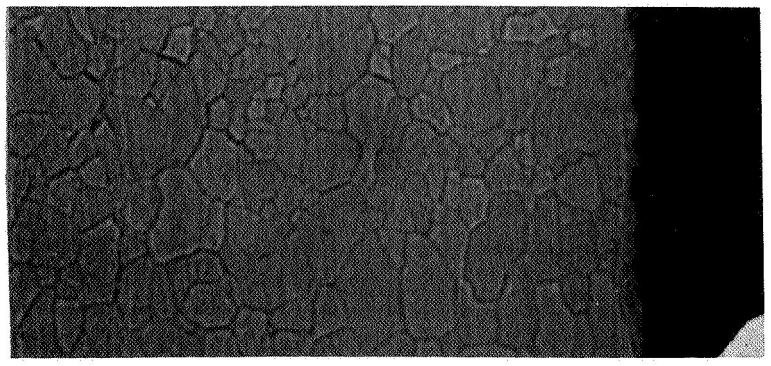

16 Hrs/2000 F

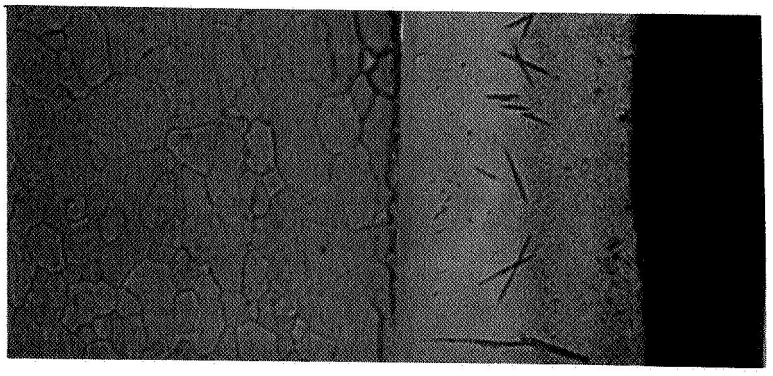

16 Hrs/2000 F
Plus Ti

FIGURE 22. STRUCTURE OF T222 ANNEALED AT 2000 F WITH AND WITHOUT A TITANIUM SINK (500X Magnification)

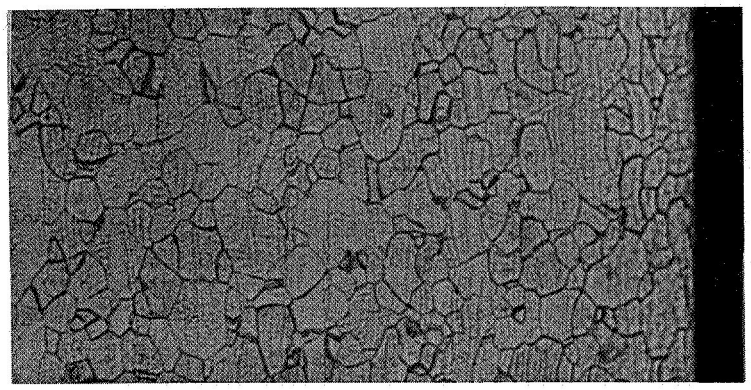

1 Hr/2500 F

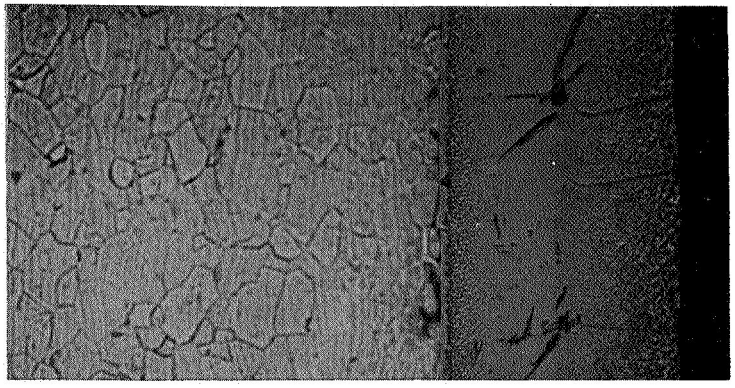

1 Hr/2500 F
Plus Ti

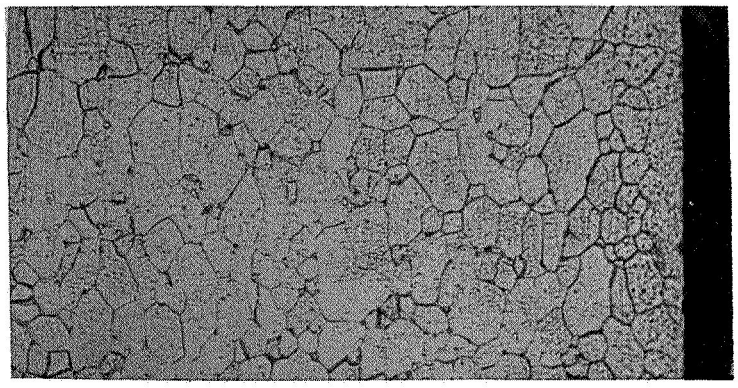

16 Hrs/2500 F

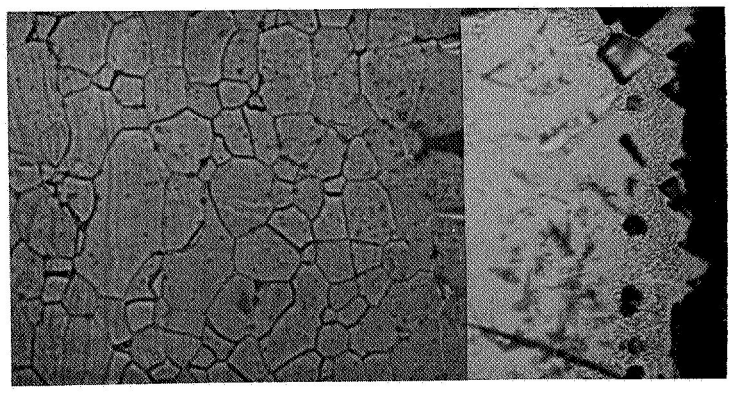

16 Hrs/2500 F
Plus Ti

FIGURE 23. STRUCTURE OF T222 ANNEALED AT 2500 F WITH AND WITHOUT TITANIUM SINK (500X Magnification)

The effects of the annealing treatments on the carbon concentration in the TZM are shown plotted in Fig. 24. The carbon concentration in the alloy is only slightly reduced at 2000° F but is reduced to less than half of its initial concentration by the longer heat treatments at 2500° F (or the 16 hour heat treatment at 2700° F, Table VII).

As shown in Table VII, the oxygen concentration in the T222 remains about the same or is slightly increased by the annealing treatments, both with and without titanium. The oxygen increase, however, is somewhat greater when the alloy is annealed without titanium bonded to its surfaces. Although the scatter in the analyses for oxygen in this low concentration range is relatively high ($\pm \sim 10$ ppm) the results are sufficiently accurate to show that titanium is not likely to be an effective interstitial sink for the oxygen that is in T222 at temperatures up to 2700° F.

The carbon concentration in T222 is not significantly reduced by annealing this alloy at 2000° F, 2500° F or 2700° F, with or without titanium; rather, the results indicate that the carbon concentration may be increased by annealing. This is evident in Table VII and in Fig. 25 where the analyses for carbon in T222 are plotted versus annealing time at 2000 and 2500° F. These analyses are certainly sufficient to show

TABLE VII

CARBON AND OXYGEN CONCENTRATIONS IN TZM AND T222 ANNEALED WITH AND WITHOUT A TITANIUM SINK

	TZM		T222	
	Analyses (ppm)		Analyses (ppm)	
Treatment	O	C	O	C
As Received	40	260	21	185
1 hr/2000° F No Ti	21	220	61	150
Plus Ti	13	200	25	157
16 hrs/2000° F No Ti	26	222	22	168
Plus Ti	25	220	28	152
1 hr/2500° F No Ti	31	177	72	183
Plus Ti	22	210	22	150
16 hrs/2500° F No Ti	23	100	98	200
Plus Ti	25	90	46	197
70 hrs/2500° F No Ti	7	75	52	320
Plus Ti	19	85	—	275
16 hrs/2700° F No Ti	25	80	60	450
Plus Ti	15	70	40	175

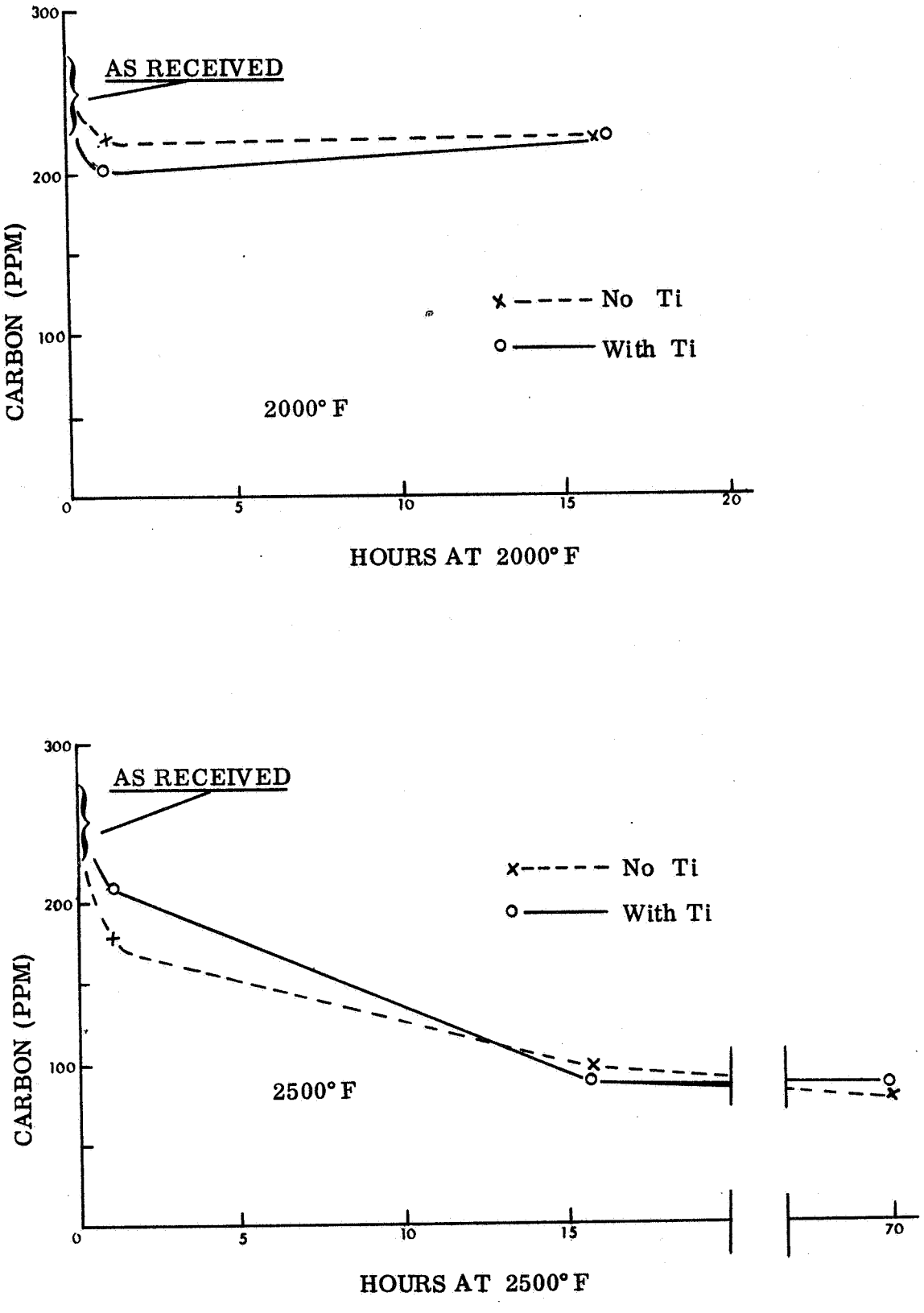

FIGURE 24. CARBON CONCENTRATION IN TZM AS A FUNCTION OF ANNEALING TIME AT 2000° F AND 2500° F

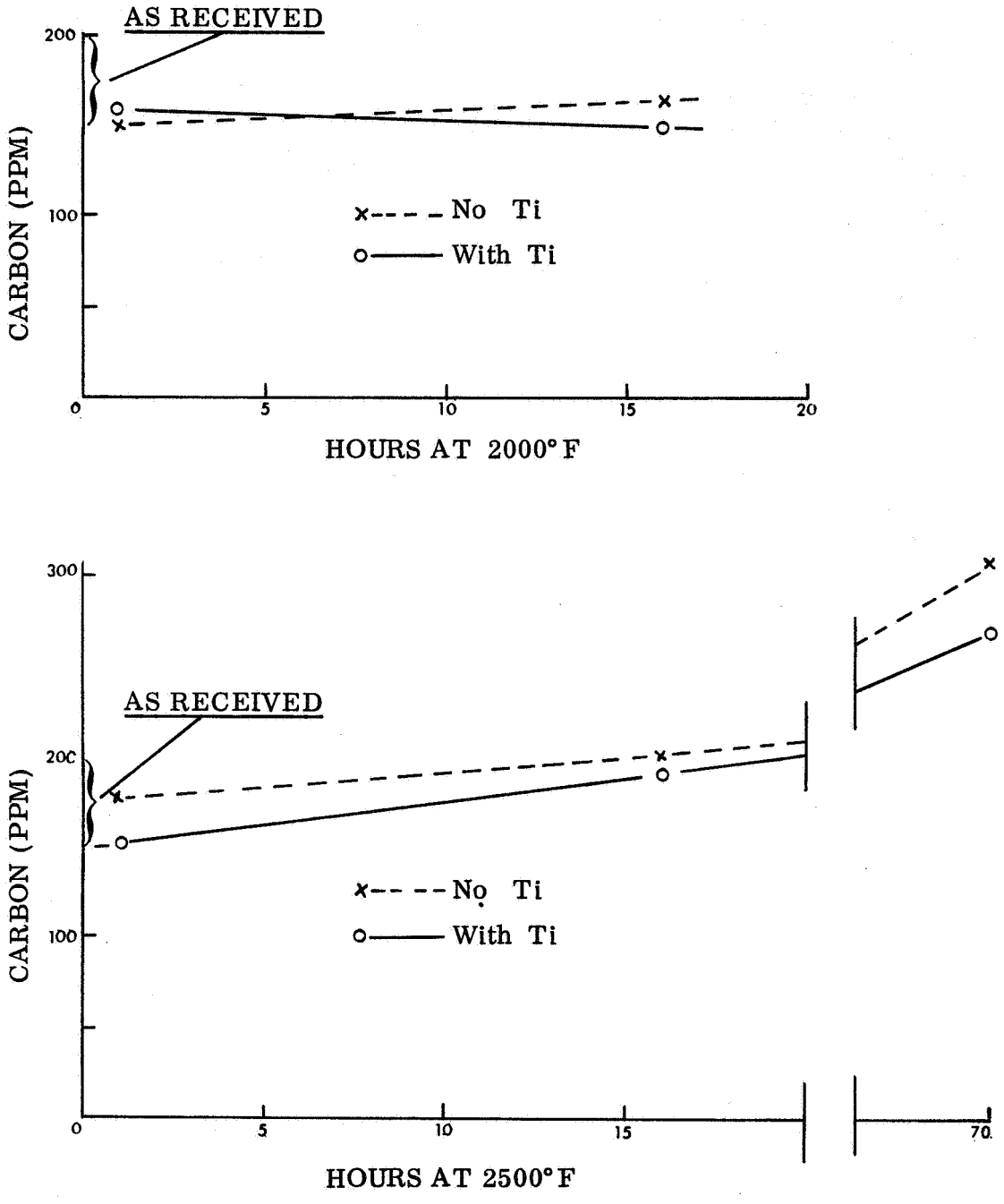

FIGURE 25. CARBON CONCENTRATION IN T222 AS A FUNCTION OF ANNEALING TIME AT 2000° F AND 2500° F

that the carbon concentration in T222 is not reduced by the action of titanium or of a vacuum for temperatures up to 2700°F. In addition, two heat treatments, 70 hour - 2500°F and 16 hour - 2700°F, show an increase in carbon concentration of the T222 when heated without titanium and one analysis, 70 hours - 2500°F, shows an increase in carbon concentration of the T222 when heated with titanium. This suggests that T222 may be susceptible to carbon pick-up during the vacuum heat treatment.

The equilibrium partition of interstitials between a refractory metal and a sink metal is determined by the difference between the partial molar free energy (μ) of the interstitials in the two metals. As previously discussed, (μ) can be defined by the equation

$$\mu = \Delta F + RT \ln X/S$$

where ΔF is the free energy of the interstitial solution for unit interstitial activity (approximated by the free energy of formation of the interstitial compound), X is the concentration of interstitial in solution in the metal, T is the temperature, and S is the saturation solubility. For two metals such as A and B where the partition of interstitial, X, has reached equilibrium (i.e., $\mu_{(x \text{ in } B)} = \mu_{(x \text{ in } A)}$) it has been shown that (First Interim Technical Report)

$$\Delta F_{AX} - \Delta F_{BX} = RT \ln \frac{S_A}{S_B} \cdot \frac{X_B}{X_A}$$

and

$$X_B/X_A = S_B/S_A \exp (\Delta F_{AX} - \Delta F_{BX})/RT \quad . \tag{14}$$

According to Eq. 14 the factors affecting the equilibrium partition, X_B/X_A at constant temperature are the saturation solubility ratio S_B/S_A for the interstitials in the two metals, and the difference in the free energies of formation of the interstitial compounds ($\Delta F_{AX} - \Delta F_{BX}$).

Available thermodynamic data suggest that titanium is qualitatively a strong sink for oxygen in both molybdenum and tantalum (the base metals for TZM and T222 respectively). It is difficult to predict the equilibrium partition of oxygen between titanium and these metals quantitatively because the thermodynamic data are not known with sufficient accuracy to permit an accurate calculation of X_B/X_A from Eq. 14. The equilibrium partition of oxygen between titanium and TZM, O_{Ti}/O_{TZM}, can be approximated, however, from the data in Table VII and the initial oxygen concentration in the titanium. The equilibrium or final oxygen concentration in the TZM after annealing the alloy with titanium at 2500 and 2700°F is almost the same as the initial concentration (~40 ppm), and the initial oxygen concentration in the titanium is about 3000 ppm. Therefore, the partition ratio, O_{Ti}/O_{TZM}, is about 100/1. Similarly, if the equilibrium oxygen concentration in the T222 is taken to be about 50 ppm

(Table VII), the partition ratio O_{Ti}/O_{T222} is about 60/1. Because of the low initial oxygen concentration in both TZM and T222 (20-40 ppm) and the relatively high initial concentration in the titanium ($\sim$3000 ppm) the initial and equilibrium partitions between the titanium and the alloys appear to be approximately equal. In this regard, the oxygen analyses in Table VII suggest that the titanium may even lose some of its oxygen to the T222 in adjusting the initial to the equilibrium oxygen ratios. The results shown in Table VII also suggest that the vacuum may be a sink for oxygen in TZM. Calculations indicate that a vacuum of about 10^{-8} Torr is required to induce a loss of oxygen in TZM through the dissociation of MoO_2 at 2500°F. However, a loss of oxygen from the TZM to the vacuum could occur by the reduction of a more unstable oxide phase that may form in this alloy or through a carbon-oxygen reaction. As shown in Table VII, the T222 may gain rather than lose oxygen as a result of vacuum annealing without titanium. This can be predicted qualitatively on the basis of the greater stability of tantalum oxide relative to molybdenum oxide (e.g., vacuum of 10^{-15} Torr would be required to dissociate Ta_2O_5 at 2500°C).

An analysis of thermodynamic data suggests that titanium will be qualitatively a strong sink for carbon in molybdenum and tantalum. However, thermodynamic data do not permit a quantitative determination of the partition of carbon between the titanium and the alloys, TZM and T222. Approximate equilibrium partitions can again be derived from the data in Table VII, the initial carbon concentration and the thicknesses of the titanium foil and alloy sheet. For initial and final carbon concentrations in the TZM of 260 and 90 ppm respectively (see Table VII) and 50 ppm carbon in the titanium, it can be shown that the final carbon concentration in the titanium must be about 3000 ppm. On this basis the equilibrium carbon ratio C_{Ti}/C_{TZM} is about 30/1.

With the exception of the 70-hour heat treatment at 2500°F, T222 shows little change in carbon concentration when heated in contact with titanium. For example, after the 16-hour heat treatments at 2500 and 2700°F with titanium, the carbon concentration in the T222 is almost the same as its initial carbon concentration. Therefore, the initial partition of carbon between T222 and titanium is almost equal to the final partition or $C_{Ti}/C_{T222} \simeq 500/200 \simeq 2.5/1$ (the initial concentration of carbon in the titanium foil is about 500 ppm).

3.2 RECRYSTALLIZATION STUDY AFTER ANNEALING WITH A TITANIUM SINK FOLLOWED BY DEFORMATION

To further investigate the effect of a titanium interstitial sink on the recrystallization kinetics of T222 and TZM, the as-received specimens that had been annealed for 16 hours at 2500°F with titanium and specimens that had been annealed without titanium were cold rolled to 75 percent reduction in area and subsequently re-annealed to induce recrystallization. The recrystallization kinetics of the titanium-annealed specimens were then compared with the recrystallization kinetics for specimens that had not been annealed with titanium prior to reduction in area.

The structures of the TZM and T222 after cold rolling are shown in Fig. 26, and the structures induced in the alloys by annealing the cold rolled specimens at temperatures from 2000 to 2500°F are shown in Figures 27 and 28. The structures of the alloys after cold rolling (Fig. 26) are typical of highly worked metals, and the structures shown in Figures 27 and 28 depict the various stages of recrystallization. The structures in the first column of these figures (labeled without Ti) are those for the as-received alloy annealed for 16 hours at 2500°F prior to a reduction in area of 75 percent and the annealing treatments indicated. The structures in the second column in these figures (labeled with Ti) are those for the Ti/alloy/Ti diffusion couples annealed for 16 hours at 2500°F prior to a reduction in area of 75 percent and the annealing treatments indicated. If interstitial partition to the titanium sink affects the recrystallization kinetics of these alloys relative to vacuum annealing without titanium the grain structures shown in the first columns should be different from those shown in the second columns of Figures 27 and 28. Since the structures are very similar, these results suggest that a titanium sink does not significantly affect the recrystallization kinetics of these alloys.

3.3 THE EFFECT OF A HAFNIUM SINK ON THE STRUCTURE OF T222

The results of Sec. 3.1 and 3.2 show that titanium (75A) does not appear to be an effective interstitial sink for the interstitials in T222. As discussed in Sec. 3.1, titanium may not have a great enough affinity for interstitials to reduce their concentrations below that initially in the T222. In order to test this hypothesis, a stronger interstitial sink, hafnium, was selected for additional study. The free energies of formation of both the oxides and carbides for this metal are judged to have a greater negative value than those for titanium (Ref. 5, 6).

The experimental procedures followed in this phase of the investigation were the same as those used for the titanium sink work described above. The structures of the as-bonded diffusion couples were very similar to those shown in Fig. 19 for T222/Ti. As previously observed, the grain structure of the T222 was not changed by the diffusion bonding. The Hf/T222/Hf diffusion couples were vacuum annealed at 2700°F for 16 hours to allow interstitial partition to take place between the two metals. Specimens of unbonded T222 were also heat treated with the diffusion couples to use as a standard for comparison of the effect of the hafnium sink on the grain structure of the alloy. The structures of specimens heated with and without a hafnium sink are shown for comparison in Fig. 29. It is evident that the alloy has a larger grain size when it is heated with hafnium. This is consistent with a reduction in the amount of grain stabilizing interstitial phase due to the action of the hafnium sink. In addition, the sink treated specimen appears to have less second phase particles at the grain boundaries. In this regard, the amount of second phase appears to be greater near the surface of the specimen heated without hafnium. This may be caused by interstitial "pick-up" during the vacuum heat treatment. As shown in Table VII, both the oxygen and carbon concentrations of the T222 are increased when the alloy is heated at 2700°F without an interstitial sink. However, if interstitial contamination has

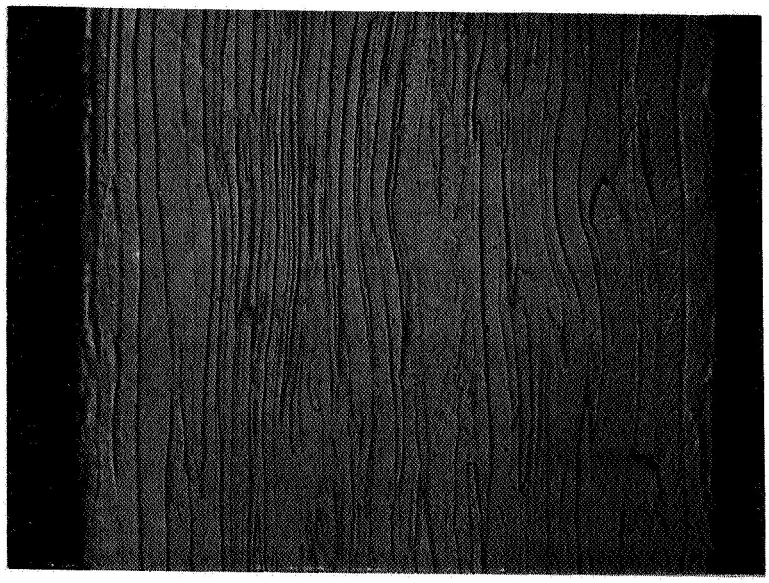

TZM

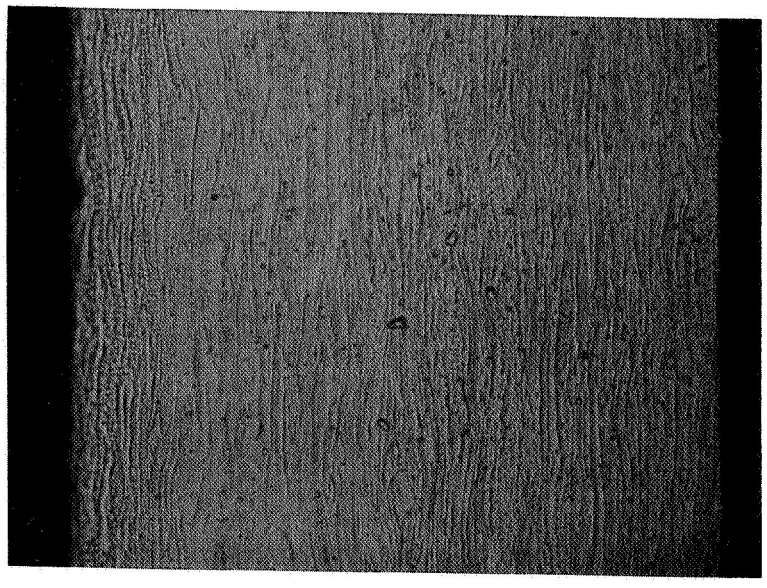

T222

FIGURE 26. STRUCTURES TYPICAL OF TZM and T222 AFTER 80 PERCENT REDUCTION IN AREA: 500 X MAGNIFICATION

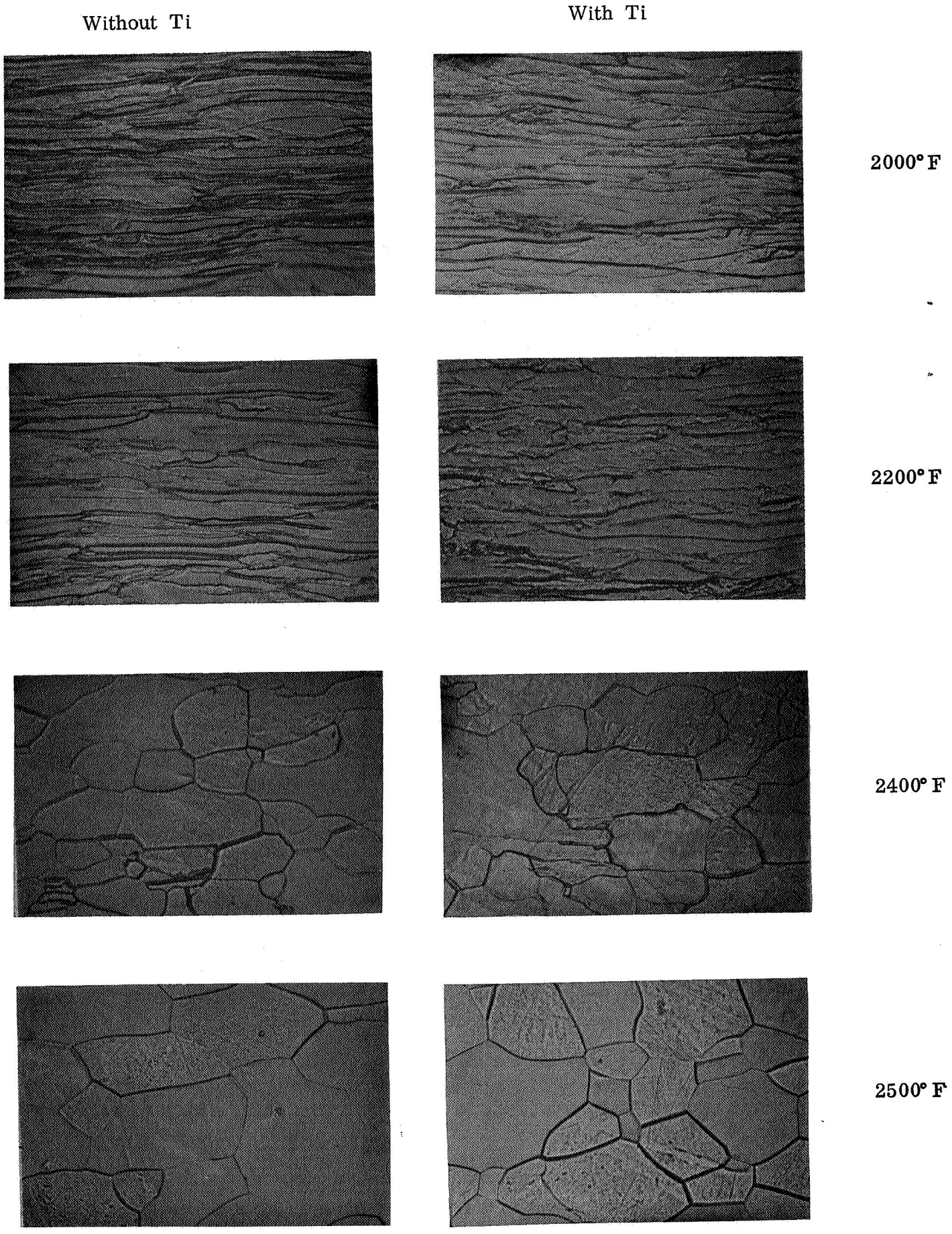

FIGURE 27. STRUCTURE OF TZM (Annealed 2500° F for 16 Hours With and Without Titanium Sink Prior to Cold Rolling and Annealing 1 Hour at the Temperatures Indicated) 500X Magnification

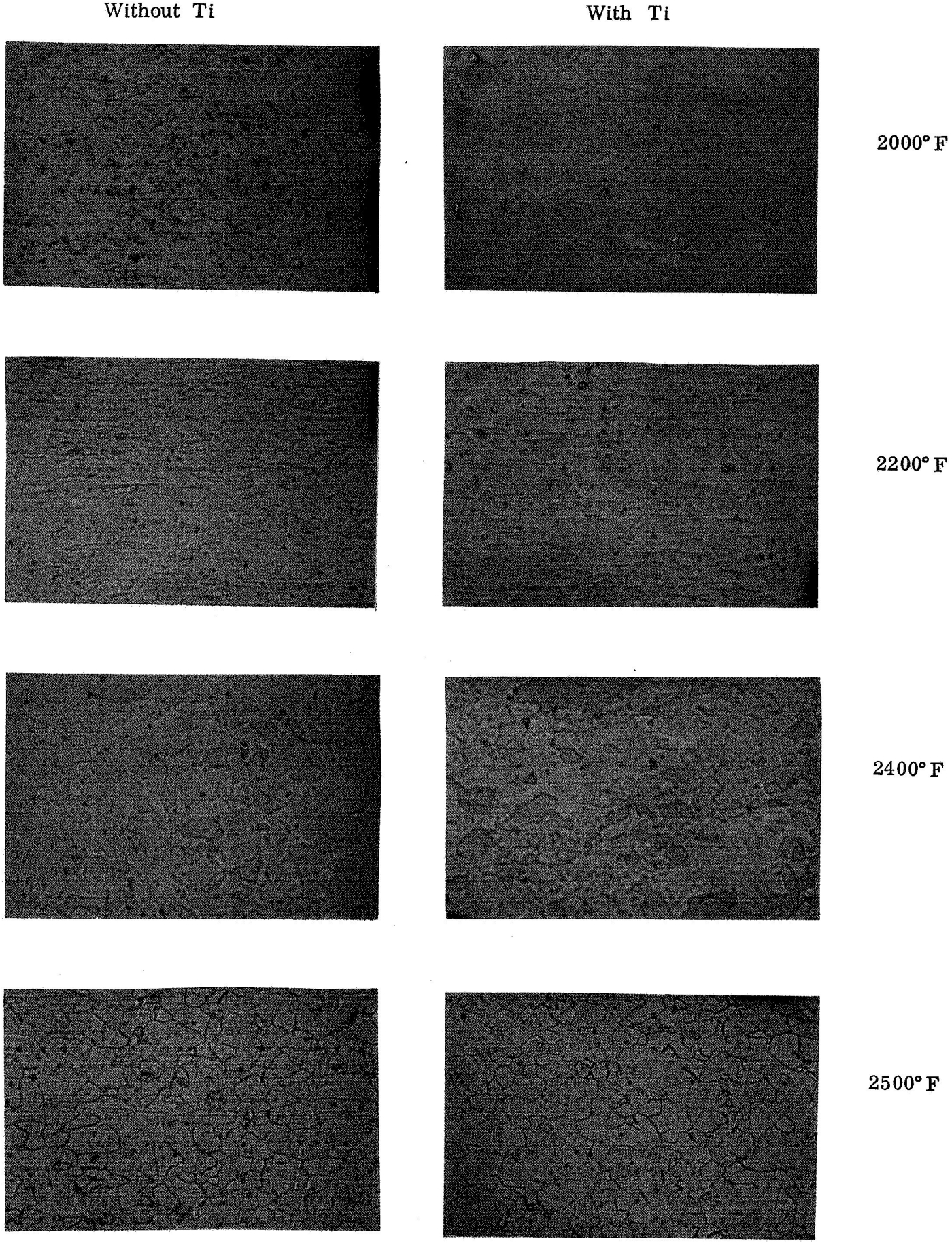

FIGURE 28. STRUCTURE OF T222 (Annealed 2500°F for 16 Hours With and Without a Titanium Sink Prior to Cold Rolling and Annealing 1 Hour at the Temperatures Indicated) 500X Magnification

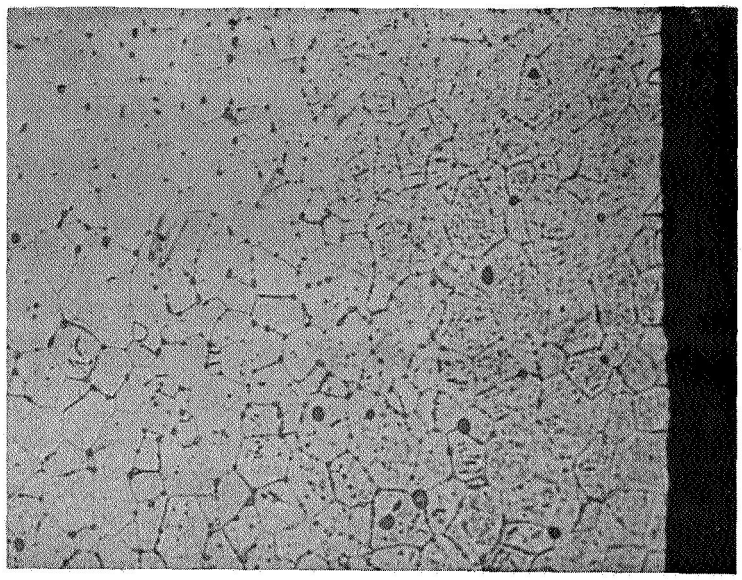

1 Hr/2700° F
Without Hf

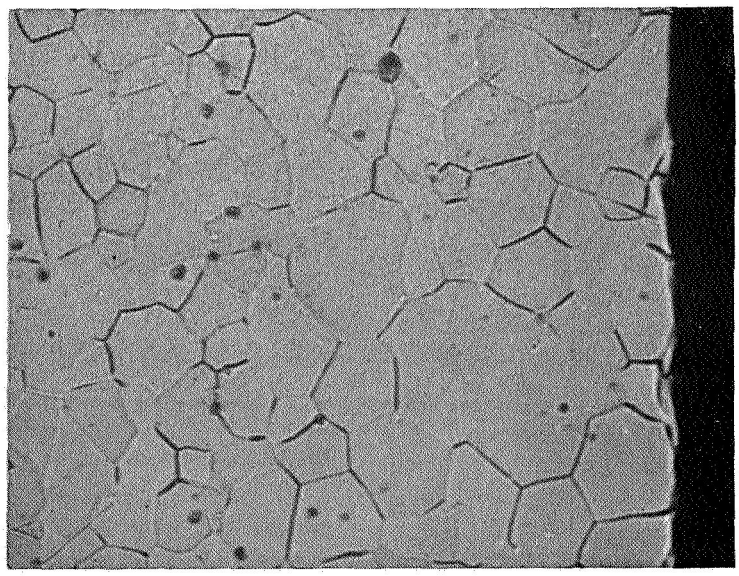

1 Hr/2700° F
With Hf

FIGURE 29. STRUCTURE OF AS-RECEIVED T222 ANNEALED AT 2700° F WITH AND WITHOUT A HAFNIUM SINK (500X Magnification)

taken place near the specimen surface, it does not seem to have affected grain growth since the grain size is uniform throughout the specimen.

Following the procedure used previously for titanium, the as-received specimens that had been annealed for 16 hours at 2700°F with hafnium and specimens that had been annealed without hafnium were cold rolled to 75 percent reduction in area and subsequently re-annealed to induce recrystallization. The grain structure of the hafnium-annealed specimens were then compared with the grain structure of specimens that had not been annealed with hafnium prior to reduction in area. Fig. 30 (A, C, D, F) shows the resulting grain structures. The specimens heated with hafnium (Fig. 30, C and F) are more fully recrystallized or have a somewhat larger grain size than those heated without hafnium (Fig. 30, A and D). For comparison of the relative effects of titanium and hafnium sinks on the grain structure of T222, the microstructures of specimens heated with titanium are also shown in Fig. 30 (B and E). It is evident that titanium has less effect on the grain structure of T222 than does hafnium.

The results of this series of tests suggest that hafnium has a great enough affinity for the interstitials in T222 to reduce the concentrations of structure stabilizing interstitial compounds (primarily carbides). This reduction in the amount of the dispersed interstitial phase is sufficient to enhance recrystallization and grain growth in this alloy. In contrast with this behavior, titanium does not appear to be an effective interstitial sink for T222.

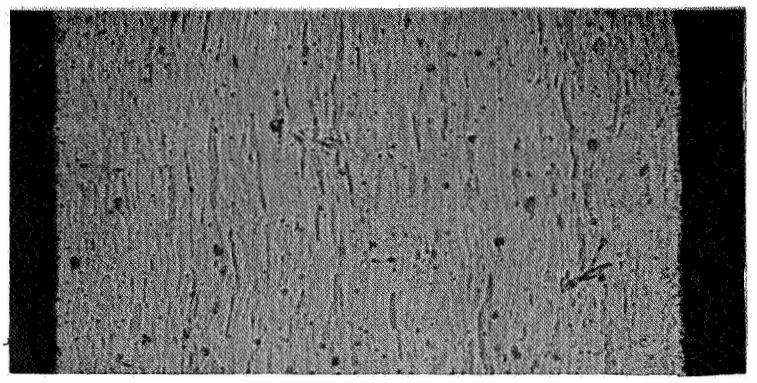

A

Heated Without Sink before Deformation and Annealing 1 Hr at 2200° F

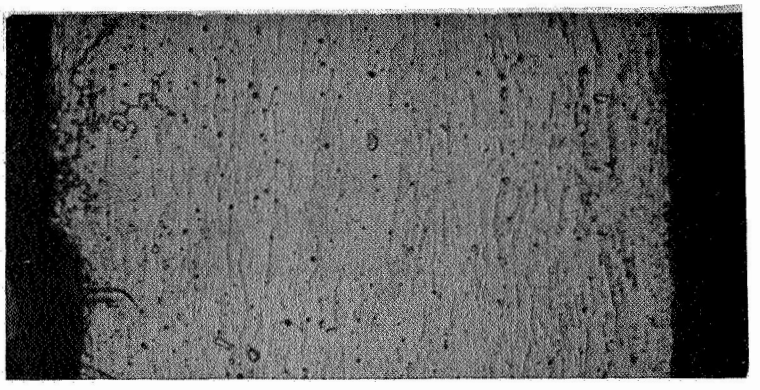

B

Heated With Ti Sink before Deformation and Annealing 1 Hr at 2200° F

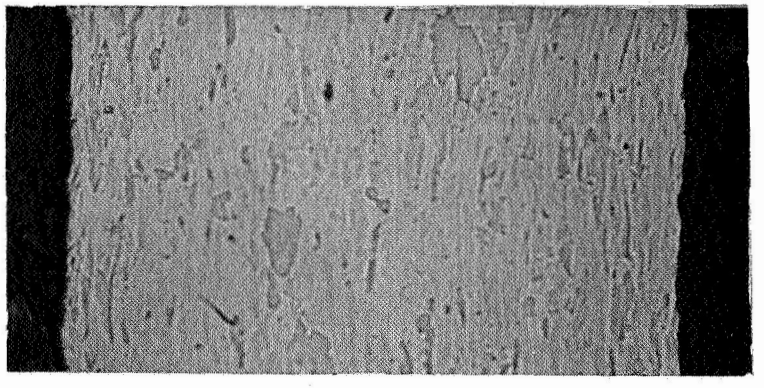

C

Heated With Hf Sink before Deformation and Annealing 1 Hr at 2200° F

FIGURE 30. STRUCTURE OF T222 HEATED WITH AND WITHOUT A SINK PRIOR TO COLD ROLLING AND ANNEALING AT THE TEMPERATURES INDICATED: 500X Magnification (Sheet 1 of 2)

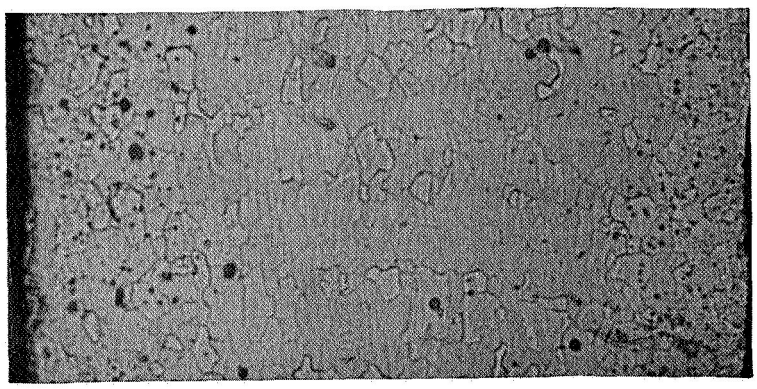

D

Heated Without Sink before Deformation and Annealing 1 Hr at 2500° F

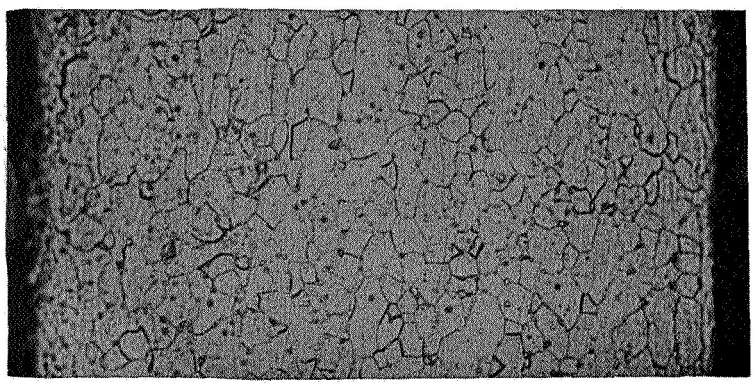

E

Heated With Ti Sink before Deformation and Annealing 1 Hr at 2500° F

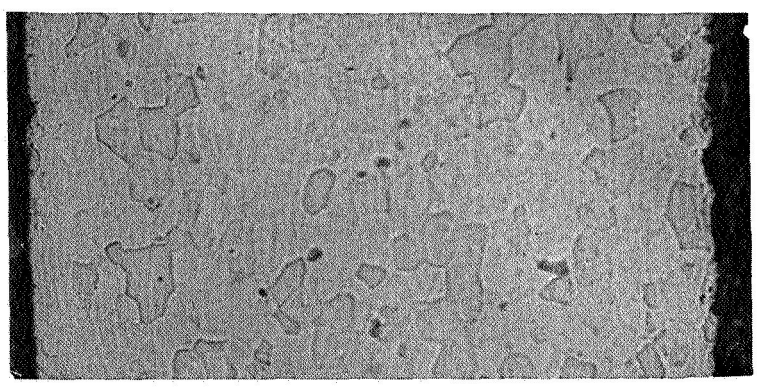

F

Heated with Hf Sink before Deformation and Annealing 1 Hr at 2500° F

FIGURE 30. STRUCTURE OF T222 HEATED WITH AND WITHOUT A SINK PRIOR TO COLD ROLLING AND ANNEALING AT THE TEMPERATURES INDICATED: 500X Magnification (Sheet 2 of 2)

IV. CHEMICAL POTENTIAL MEASUREMENTS

A method to determine the chemical potential of interstitials in refractory alloys was evaluated. The objective was to generate experimental interstial-partition data for comparison with partitions calculated from thermodynamic data (Sec. II, First Interim Technical Report). The system selected was oxygen in columbium-titanium alloys, a system comparable with Ti/D43. The procedure followed was similar to that used by Kubaschewski, et al, (Ref. 7), and Allen, et al, (Ref. 8) to determine the partial free energy (chemical potential) of oxygen in titanium and vanadium with one major exception; in the present study foil specimens were used, whereas in the previous work powder specimens were used. It was believed that the foil specimens would minimize difficulties encountered in the referenced works in separating the specimens from the calcium in which they were embedded.

Foil specimens (0.010 in. thick) of Ti, Ti-50Cb and Cb were placed in titanium bombs containing calcium. The bombs were evacuated and heated at 1200° C to allow oxygen to partition between the calcium and the foil specimens. After this heat treatment, the calcium was chemically removed from the foils and the residual oxygen in the foils was analyzed. It was assumed that equilibrium was attained and that

$$\mu_{M(O)} = \Delta F^{\circ}_{CaO}$$

where $\mu_{M(O)}$ is the chemical potential of oxygen in the foils and ΔF° in the free energy of formation of CaO at the heat treating temperature. Since ΔF°_{CaO} is known (115K Cal/Mole), it follows that $\mu_{M(O)}$ can be determined for the reduced oxygen concentrations in the foils.

The results of the analysis are listed in Table VIII. Tests were made using duplicate bombs to check the reproducibility of the experimental techniques and the analysis. One bomb was tested using a powder specimen rather than a foil specimen. This was done to compare the residual oxygen analysis for similarly treated powder and foil specimens. As shown in Table VIII, the oxygen concentration in the powder specimen (Bomb 3) is much greater than that in the foil specimens, (Bombs 1 and 2). High oxygen values could result from incompleteness of the reaction in the bomb and oxygen pick-up during treatment of the powder after removal from the bomb. Incompleteness of the reaction for the powder material could be a factor contributing to its greater residual oxygen concentration since its initial oxygen concentration was higher than that of the titanium foil. On the other hand, the much greater area of contact of the powder specimens with the calcium should facilitate rapid partition of oxygen. It is, therefore, more likely that oxygen pick-up during or after separation of the powder from the calcium is a major factor contributing to its high oxygen concentration.

TABLE VIII

REDUCTION IN OXYGEN CONCENTRATIONS INDUCED BY CALCIUM

Bomb No.	Foil Composition	Oxygen Concentration (ppm)
1	Ti	870
2	Ti	920
3	Ti (Powder)	4370
4	Ti-50 at% Cb	240
5	Ti-50 at% Cb	250
6	Cb	130
7	Cb	105

In this regard, high values of oxygen in similarly treated vanadium and titanium powders in the referenced works were attributed to oxygen pick-up after the equilibrium heat treatment. For titanium powder equilibrated with calcium at ~1000° C oxygen concentrations ranging from 700 to 1200 ppm were reported (Ref. 7). Because of possible oxygen contamination, the low concentration, 700 ppm, was taken as the best value.

As shown in Table VII, the agreement between oxygen concentrations for the duplicate specimens is good, showing that the experimental methods are reproducible. In addition, the much lower oxygen concentration in the foil specimen relative to the powder specimen suggests that the former are preferable to minimize oxygen pick-up in this type of experiment. The concentration of residual oxygen in the specimens decreases progressively in the order Ti, Ti-50Cb, and Cb. This is in agreement with the theory predicting a much greater oxygen affinity for titanium relative to columbium. However, the residual oxygen concentrations listed in Table VIII are much greater than the equilibrium values calculated according to Eq. 10 (e.g., 12 ppm oxygen in titanium). Additional work would be required to ascertain the cause of the discrepancy between the experimental and calculated values, and this is beyond the scope of the present program.

V. SUMMARY AND CONCLUSIONS

This investigation is a study of the relationships between the interstitial concentration, the structure and the creep strength of refractory metals when they are subjected to an interstitial sink (a metal in which interstitials concentrate). The system studied in greatest detail thus far is that for carbon partition between a titanium (or titanium-columbium) sink and a columbium base alloy, D43.

5.1 CREEP OF D43

The activation energy for creep of the as-processed D43 was determined from 1600 to 3200°F. Above about 2200°F the activation energy is approximately equal to that for self-diffusion and is independent of temperature and stress. These characteristics suggest that the rate controlling creep mechanism in this temperature range involves dislocation climb. Examination of the structures before and after creep suggest that the rate controlling mechanism is the climb of edge dislocations over carbide particles.

Creep studies at 2200°F show that the activation energy is also relatively independent of creep strain, the processing treatment and precreep treatments that produce gross changes in the structure of the alloy; heat treatments that reduce the dislocation and subgrain density and interstitial sink treatments that remove the carbide dispersion produce only minor changes in the activation energy for creep. Therefore, creep appears to be controlled by a dislocation climb mechanism independent of the carbide dispersion and the dislocation structures in this alloy. Below about 2200°F preliminary results indicate that the activation energy for creep increases to values above that for self-diffusion. This increase in the activation energy is believed to be caused by solute-atom dislocation interactions in this temperature range.

The stress dependency of the strain rate at 2200°F for D43 processed in different ways ranges from $n = 7.7$ to 9.5 where $\dot{\epsilon} \alpha \sigma^n$. In addition, the stress exponent, n, is relatively independent of precreep treatments that change the structure of the alloy. Heat treatments both with and without an interstitial sink produced little change in the stress exponent. Yet, these treatments eliminate the subgrain structure, the carbide dispersion and reduce the dislocation density.

The stress exponent for the high temperature creep of many pure metals (BCC, FCC and HCP structures) is about five (Ref. 9). Data have been reported showing a tendency for solute additions to decrease the stress sensitivity (Ref. 10) and for a dispersed phase to increase the stress sensitivity. For the latter case, values of n up to 40 have been reported (Ref. 11). Although the data available are rather meager, most of the dispersion strengthened alloys investigated show stress

exponents in the range 6 to 8 (Ref. 4), (e.g., Al_2O_3-Ni, Al_2O_3-Al and ThO_2-Ni). Thus, the range of values for D43 of 7.5 to 9.5 is near the range of values found in a number of other systems.

In previous work attention has been drawn to a correlation between the stored energy of cold work and the stress exponent for dispersioned strengthened alloys. Increasing values of n were correlated with an increase in the amount of deformation to which the alloy was subjected and a decrease in the grain or subgrain size. For example, the stress exponent for recrystallized ThO_2-Ni was found to be in the range 6 to 8 (Ref. 4), whereas the stress exponent for the as-processed alloy with a more worked structure was 40 (Ref. 11). The results for D43, however, show no such correlation. Differences in processing result in only minor changes in the stress exponent. In this regard, D43 (Dup F) which is the processing condition showing the most annealed structure (i.e., largest subgrain size and lowest dislocation density), has a somewhat larger stress exponent than D43 processed in the other conditions (n = 9.5 versus n = 8.1 and 7.7). In contrast with the results cited for ThO_2-Ni, the stress exponent for D43 appears to be independent of structure. Interstitial sink treatments that change the structure before creep (Fig. 17) and also affect a change in the structure after creep (Fig. 18) have little influence on the stress exponent (Table VII).

Ansell and Weertman (Ref. 12) have derived theories for the creep of dispersion strengthened alloys. For fine grained or as-processed SAP alloy they propose that the stress dependence of the creep rate is in the activation energy term. Thus $\dot{\epsilon} \propto \exp. -\frac{(H - B\sigma)}{RT}$ where B is a constant. For this qualitative relationship it is proposed that the creep rate is controlled by the rate of dislocation generation from grain boundaries.

The as-processed D43 does not obey a relationship of this type since the measured activation energy is constant in the range 2200-3200°F and is independent of stress. For recrystallized or coarse grained dispersion strengthened alloys their theory predicts that $\dot{\epsilon} \propto \sigma$ for low stress, $\dot{\epsilon} \propto \sigma^4$ for intermediate stress, $\dot{\epsilon} \propto \sigma^2 \exp \sigma^2$ for high stress. These derivations are based upon a strain rate controlled by the climb of edge dislocation over second-phase particles. None of these stress dependencies agree with the data derived for D43, whether fully annealed or as-processed.

The stress dependence of the creep rate, σ^n, has also been related to the stress dependence of the mobile dislocation density, σ^δ (Ref. 13). Thus $\dot{\epsilon} \propto \sigma^n \propto \sigma^\delta$ so that for a given stress an increase in δ increases both $\dot{\epsilon}$ and n. Further, it has been proposed that

$$\frac{2\sigma}{\sigma - \sigma^\circ} = \delta$$

where $\sigma_\circ$ is termed a friction stress or internal resistance to dislocation movement. As $\sigma_\circ$ increases δ will increase and so, therefore, will the stress exponent n. It has been suggested that $\sigma_\circ$ will be large for dispersion strengthened metals and that

this accounts for stress exponents greater in dispersion strengthened alloys than in pure metals. According to this concept, the stress exponent, n, should decrease upon removal of the dispersed phase. However, the results of this study show that the stress exponent is not changed by the progressive removal of the carbide phase by the interstitial sinks.

The stress dependence of the creep rate of D43, therefore, cannot be correlated with existing creep theories. It is independent of structure and has a value somewhat larger than that found for pure metals.

The results of this study of the creep behavior of D43 show that the creep rate near 0.5 T_M can be expressed empirically by the equation

$$\epsilon^{\circ} = A \sigma^{n} e^{-H/RT}$$

where H is 112 - 118 K cal/mole (approximately that for self-diffusion), n is 7.7 to 9.5 and A is $(1.7 \times 10^{-2})/C$. The term, C, included in the definition of A is the concentration of carbon in the alloy in ppm from 100 ppm to the maximum carbon concentration tested, 800 ppm. An interstitial sink reduces the carbon concentration in the D43, thereby increasing the value of A and the creep rate. The values of n and H do not appear to be affected by the action of the interstitial sink. Structure studies show that the reduction in carbon induced by the interstitial sinks corresponds with a reduction in the number of carbide particles that obstruct dislocation movement. As these obstructions are removed by the sink, the creep rate increases.

The subgrain and dislocation structures in D43 introduced during processing and during creep do not, in themselves, seem to play an important role in strengthening this alloy. The results suggest rather that the obstructions offered by carbide particles to moving dislocations during creep contribute more to the high temperature strength of this alloy. In this regard, electron microscopy observations of specimens after creep testing at 2200° F show little evidence of substructure retention or formation; however, these specimens do show a high degree of direct interaction of dislocations with carbide particles. The effect of processing treatment on the creep rate (a change in creep rate by a factor of 2 to 3) is believed to be caused at least in part by the variations in the carbide particle distribution and size in the differently processed specimens. Substructure may be a factor influencing the nucleation and growth of the carbides in D43 during processing and thus may indirectly affect the creep rate by influencing the characteristics of the carbide.

The importance of carbides to the high temperature strength of D43 is shown by the increase in creep rate at 2200° F by a factor of about 20 for a decrease in carbon concentration of about 700 ppm. This reduction in carbon concentration is directly proportional to the affinity of the interstitial sink for the carbon in D43. The reduction in carbon in the alloy can be correlated qualitatively with a reduction in the number of

carbide particles (and, therefore, an increase in interparticle spacing) rather than with a reduction in the diameter of the particles. On this basis, the proportionality between creep rates of the sink treated specimens and their reciprocal carbon concentrations can be accounted for.

5.2 EFFECTS OF INTERSTITIAL SINKS ON TZM AND T222

The effects of a titanium sink on the interstitial concentration and the recrystallization behavior of TZM and T222 in the temperature range 2000-2700° F were studied. The recrystallized grain structures of these alloys did not differ significantly for specimens annealed with and without a titanium sink. The carbon concentration in the TZM was reduced to less than half of its initial concentration when the alloy was vacuum heat treated at 2500 and 2700° F. This reduction occurred when the alloy was heat treated with titanium or without titanium; thus, vacuum heat treatments were about as effective as titanium in removing carbon from TZM. However, neither the vacuum heat treatments nor the action of titanium were effective in removing carbon or oxygen from T222. Results thus far have shown that titanium more effectively removes carbon and oxygen from D43 than from TZM. Titanium does not appear to be an effective sink for the interstitials in T222. However, the results of a study of the recrystallization behavior of T222 subjected to a hafnium sink suggest that this reactive metal is a sink for interstitials in T222.

5.3 CHEMICAL POTENTIAL MEASUREMENTS

An experimental method to determine the chemical potential of interstitials in refractory metals was investigated. The experimentally measured partition of oxygen in titanium-columbium alloys for a given chemical potential was compared with the partition determined from thermodynamic calculations. Agreement was good qualitatively but poor quantitatively. Although this method has good potential, additional work would be required to critically evaluate its capabilities.

VI. FUTURE WORK

The creep rate is related to the activation energy by an exponential term, exp-H/RT. Therefore, the creep rate is a sensitive function of the magnitude of the activation energy for creep. Above about $0.5T_M$ the activation energy is approximately constant and is usually equal to that for self-diffusion. One way in which the activation energy for creep can be increased above that for self-diffusion is to develop an alloy in which a solute-dislocation interaction creates a stable dislocation atmosphere. Here, the activation energy becomes that required to move the entire atmosphere rather than that for a vacancy-atom interchange characteristic of dislocation climb. Under the conditions where the drift velocity of the atmosphere is approximately equal to the dislocation velocity, the effective activation energy may become extremely high and the creep rate correspondingly low. Examples of this behavior are Zircaloy (Ref. 14), nickel (Ref. 15), Al-3.2Mg (Ref. 16) and D43 in the present work (Fig. 2). The activation energy for creep in a certain temperature range for each metal is above the activation energy for self-diffusion. During the forthcoming period (March 8, 1968 through June 8, 1969) the creep behavior of a number of columbium and tantalum base alloys will be studied to determine the contribution of solutes to the elevated temperature strength of these alloys. The alloys will be selected to sort out the influence of various solutes on the creep rate through their effect on the activation energy. This phase of the investigation should provide valuable information that is necessary to optimize the high temperature strength of refractory alloys and increase the efficiency of alloy development.

REFERENCES

1. D. McLean, "Vacancies and Other Point Defects in Crystals," Institute of Metals, 1958, p. 159.
2. A. H. Cottrell, "Relation of Properties to Microstructures," Amer. Soc. Metals, 1954, p. 131.
3. C. S. Hartley, J. E. Steedly and L. D. Parson, "Diffusion in BCC Metals," Amer. Soc. Metals, 1965, p. 51.
4. A. H. Clauer and B. A. Wilcox, Science Jour., 1, 86 (1967).
5. A. Glassner, USAEC, ANL Rept. 5750, 1965.
6. N. E. Ryan, ARL/MET 50, 1963.
7. O. Kubaschewski and W. A. Dench, Jour. Inst. Metals, 82, 87 (1953-54).
8. N. P. Allen, O. Kubaschewski and O. von Goldbeck, Jour. Electrochem. Soc., 8, 417 (1951).
9. R. R. Vandervoort, Trans. AIME, 242, 345 (1968).
10. D. McLean, Met. Reviews, 7, 481 (1962).
11. B. A. Wilcox and A. H. Clauer, Trans. AIME, 236, 570 (1966).
12. G. S. Ansell and J. Weertman, Trans. AIME, 215, 838 (1959).
13. C. R. Barrett, Trans. AIME, 239, 1726 (1967).
14. J. J. Holmes, Jour. Nuc. Mater., 13, 137 (1964).
15. N. R. Borch, L. A. Shepard, and J. E. Dorn, Trans. ASM 52, 494 (1960).
16. P. R. Landon, L. A. Shepard and J. E. Dorn, Trans. ASM, 51, 900 (1959).